nature

https://doi.org/10.1038/s41586-022-05531-1

Accelerated Article Preview

Non-viral precision T cell receptor replacement for personalized cell therapy

Received: 16 June 2022

Accepted: 4 November 2022

Accelerated Article Preview

Cite this article as: Foy, S. P. et al. Non-viral precision T cell receptor replacement for personalized cell therapy. *Nature* https://doi.org/10.1038/s41586-022-05531-1 (2022)

Susan P. Foy, Kyle Jacoby, Daniela A. Bota, Theresa Hunter, Zheng Pan, Eric Stawiski, Yan Ma, William Lu, Songming Peng, Clifford L. Wang, Benjamin Yuen, Olivier Dalmas, Katharine Heeringa, Barbara Sennino, Andy Conroy, Michael T. Bethune, Ines Mende, William White, Monica Kukreja, Swetha Gunturu, Emily Humphrey, Adeel Hussaini, Duo An, Adam J. Litterman, Boi Bryant Quach, Alphonsus H. C. Ng, Yue Lu, Chad Smith, Katie M. Campbell, Daniel Anaya, Lindsey Skrdlant, Eva Yi-Hsuan Huang, Ventura Mendoza, Jyoti Mathur, Luke Dengler, Bhamini Purandare, Robert Moot, Michael C. Yi, Roel Funke, Alison Sibley, Todd Stallings-Schmitt, David Y. Oh, Bartosz Chmielowski, Mehrdad Abedi, Yuan Yuan, Jeffrey A. Sosman, Sylvia M. Lee, Adam J. Schoenfeld, David Baltimore, James R. Heath, Alex Franzusoff, Antoni Ribas, Arati V. Rao & Stefanie J. Mandl

Title: Non-viral precision T cell receptor replacement for personalized cell therapy

Authors: Susan P. Foy[1,13†], Kyle Jacoby[1,13], Daniela A. Bota[2,13], Theresa Hunter[1], Zheng Pan[1], Eric Stawiski[1], Yan Ma[1], William Lu[1], Songming Peng[1], Clifford L. Wang[1], Benjamin Yuen[1], Olivier Dalmas[1], Katharine Heeringa[1], Barbara Sennino[1], Andy Conroy[1], Michael T. Bethune[1], Ines Mende[1], William White[1], Monica Kukreja[1], Swetha Gunturu[1], Emily Humphrey[1], Adeel Hussaini[1], Duo An[1], Adam J. Litterman[1], Boi Bryant Quach[1], Alphonsus H. C. Ng[3], Yue Lu[3], Chad Smith[1], Katie M. Campbell[4], Daniel Anaya[1], Lindsey Skrdlant[1], Eva Yi-Hsuan Huang[1], Ventura Mendoza[1], Jyoti Mathur[1], Luke Dengler[1], Bhamini Purandare[1], Robert Moot[1], Michael C. Yi1, Roel Funke[1], Alison Sibley[1], Todd Stallings-Schmitt[1], David Y. Oh[5], Bartosz Chmielowski[4,6], Mehrdad Abedi[7], Yuan Yuan[8], Jeffrey A. Sosman[9], Sylvia M. Lee[10], Adam J. Schoenfeld[11], David Baltimore[12], James R. Heath[3], Alex Franzusoff[1], Antoni Ribas[4,6,14†], Arati V. Rao[1,14], Stefanie J. Mandl[1,14†]

Affiliations:

1. PACT Pharma, South San Francisco, CA, USA.
2. Department of Neurology and Chao Family Comprehensive Cancer Center, University of California, Irvine, CA, USA.
3. Institute for Systems Biology, Seattle, WA, USA.
4. Department of Medicine, Division of Hematology-Oncology, University of California, Los Angeles (UCLA), Los Angeles, CA, USA.
5. Division of Hematology/Oncology, Department of Medicine, University of California, San Francisco, CA, USA.
6. Jonsson Comprehensive Cancer Center at the University of California Los Angeles, Los Angeles, CA, USA.
7. Division of Hematology/Oncology, Department of Internal Medicine, University of California Davis Comprehensive Cancer Center, Sacramento, CA, USA.

8. Department of Medical Oncology and Therapeutics Research, City of Hope National Medical Center, Duarte, CA, USA.
9. Department of Medicine and Robert H. Lurie Cancer Center, Northwestern University, Evanston, IL, USA.
10. Clinical Research Division, Fred Hutchinson Cancer Research Center, Seattle, WA, USA.
11. Thoracic Oncology Service, Division of Solid Tumor Oncology, Department of Medicine, Memorial Sloan Kettering Cancer Center, Weill Cornell Medical College, New York, NY, USA.
12. Division of Biology and Biological Engineering, California Institute of Technology, Pasadena, CA, USA.
13. These authors contributed equally: Susan P. Foy, Kyle Jacoby, and Daniela A. Bota.
14. These authors jointly supervised this work: Antoni Ribas, Arati V. Rao, and Stefanie J. Mandl.

†e-mail: sfoy@pactpharma.com, ARibas@mednet.ucla.edu, smandl@pactpharma.com

Summary Paragraph

The T cell receptor (TCR) provides the fine specificity of T cells to recognize mutations in cancer cells [1-3]. We developed a clinical-grade approach based on CRISPR/Cas9 non-viral precision genome editing to simultaneously knock-out the two endogenous TCR genes, TCRα (*TRAC*) and TCRβ (*TRBC*), and insert in the *TRAC* locus the two chains of a neoantigen-specific TCR (neoTCR), isolated from the patient's own circulating T cells using a personalized library of soluble predicted neoantigen-HLA capture reagents. Sixteen patients with refractory solid cancers received up to three distinct neoTCR-transgenic cell products, each expressing a patient-specific neoTCR, in a cell dose-escalation, first-in-human phase 1 clinical trial (NCT03970382). One patient had grade 1 cytokine release syndrome, and one grade 3 encephalitis. All had the expected side effects from the lymphodepleting chemotherapy. Five patients had stable disease, and the other 11 had disease progression as best response on therapy. NeoTCR-transgenic T cells were detected in tumour biopsies post-infusion at frequencies higher than the native TCRs pre-infusion. This study demonstrates the feasibility of isolating and cloning multiple TCRs recognizing mutational neoantigens, the simultaneous knock-out of the endogenous TCR and knock-in of the neoTCRs using single-step, non-viral precision genome editing, the manufacturing of neoTCR engineered T cells at clinical grade, the safety of infusing up to three gene edited neoTCR T cell products, and the ability of the transgenic T cells to traffic to the patients' tumours.

Main Text

The ultimate goal of any cancer therapy is to target and kill cancer cells while sparing normal cells. The human immune system is uniquely suited to achieve this goal due to the fine specificity of the T cell receptor (TCR), which can distinguish single point mutations in the cancer genome that change the amino acid sequences of peptides presented by the major histocompatibility complex (MHC) on the cancer cell surface [1-4]. Mutational neoantigens provide the main target for therapeutic activity of adoptive cell transfer (ACT) of tumour infiltrating lymphocytes (TIL), antitumour T cells stimulated by immune checkpoint blockade, or cancer-specific vaccines [3-10]. Developing a clinical-grade approach to efficiently isolate multiple TCRs that specifically recognize mutated peptides presented by any of a patient's six human leukocyte antigen (HLA) class I alleles and subsequently engineer them back into autologous T cells for ACT therapy would open a new way to potentially treat refractory cancers. This goal has been limited by the large diversity of HLA class I alleles in the human population, with over 24,000 alleles currently recorded [11], and the polymorphic nature of the great majority of mutational antigenic determinants recognized by T cells [3]. This is the reason why most current TCR-engineered T cell therapies are limited to patients with HLA-A:02*01 haplotype [12]. The generation of arrays of mutated peptide-HLA TCR-binding reagents and single-cell cloning of the paired TCR chains provided a new approach to isolate neoantigen-specific TCRs (neoTCR) across multiple HLA alleles [13]. Furthermore, previous engineering of human T cells has relied on the use of recombinant viral vectors [12,14], but it is unfeasible to generate multiple personalized clinical grade vectors for every patient being treated. The advent of nuclease-based precision gene editing allowed developing approaches that use targeted insertion of transgenes into human T cells [15], and has paved the way to achieve stable integration without requiring the use of viral vectors [16]. Precision gene editing with nucleases such as CRISPR/Cas9 allows simultaneous knock-out of the endogenous TCR chains whilst inserting the transgenic TCR under the control of the physiologic TCR

promoter, which has been reported in some settings [17,18], but not all [19], to provide advantages over the same transgenes expressed under the control of constitutive viral vector promoters.

In the current study, we describe the development of a highly sensitive approach for efficient isolation of multiple TCRs specific for mutational neoantigens. This approach uses personalized libraries of hundreds of predicted neoantigen peptide sequences presented by the individual patient's HLA class I alleles, and a targeted, non-viral gene editing approach to reconstitute the specificity of the isolated neoTCRs in a time-efficient process to generate clinical-grade neoTCR-transgenic T cell preparations for ACT (**Figure 1a**). Using these technologies, we have dosed 16 patients with solid cancers with up to three unique lots of gene-engineered T cells expressing patient-specific neoTCRs targeting private mutations from their cancer.

Personalized isolation of neoTCRs

Patients consented to provide a tumour biopsy plus peripheral blood mononuclear cells (PBMC) as part of the screening for personalized neoTCR product selection (**Extended Data Figure 1a**). Germline DNA from PBMCs was compared with tumour DNA using whole exome sequencing (WES) for the identification of patient-specific tumour mutations. In addition, RNA sequencing (RNAseq) was performed to determine the level of expression of the genes with cancer-specific mutations. For the 16 patients dosed in the clinical trial, a median of 102 (range 31-488) non-synonymous somatic mutations (NSM) and a median of 35 (range 20-236) expressed mutations were identified for each patient (**Extended Data Table 1**). With this approach, we prioritized a list of up-to 352 neoantigen peptide-HLA candidates per patient (median 352, range 86-352, for a total of 5,302 peptide-HLA candidates; peptide lengths of 8 to 11 amino acids) across the available HLA class I alleles for that patient. The peptide-HLA complex libraries were produced in 293 cells as single-chain trimers, where neoantigen peptides were fused in sequence to beta-2-microglobulin (β2M) domains and the HLA. Of these, a median of 104 (range 49-262) patient-

specific peptide-HLA proteins were successfully synthesized (yield ≥ 2.7 µg) per patient for a total of 1,841 peptide-HLA proteins produced (**Extended Data Table 1**). These covered a total of 34 unique HLAs of the 64 HLA alleles represented in the screening process (**Supplementary Table 1**), with a median of 5 (range 2-6) HLA alleles covered per patient (**Extended Data Table 1**). The peptide-HLA proteins were then DNA-barcoded, fluorescently labelled and multimerized. CD8 T cells enriched from the patient's PBMCs were then stained using the patient-specific peptide-HLA multimer library to isolate rare peripheral blood-circulating T cells for any of the predicted mutations and HLA complexes, followed by single cell sorting with high sensitivity and specificity. T cell isolation included CD95 cell surface staining to exclude CD8 T cells with a naïve phenotype. Using this approach, we identified a median of 8 (range 3-30) unique TCRs from T cells of varying frequency per patient resulting in a total of 175 TCRs for the 16 patients in the clinical trial, which recognized a median of 5 (range 3-11) unique non-synonymous somatic mutations for a total of 84 neoantigen mutations (examples of typical data read-outs are given in **Figure 1b** and **1c**).

neoTCR product selection

The biological and potential therapeutic relevance of the captured candidate TCRs against the tumour neoantigens was then corroborated by precision genome engineering of healthy donor T cells with each of the patient-isolated neoTCR candidates. The TCR-alpha and -beta genes from each captured T cell were single-cell sequenced and cloned into homologous recombination (HR) DNA plasmids. These HR plasmids were used together with site-specific nucleases to knock-out the endogenous TCR-beta chain and insert the transgenic TCR-alpha and -beta genes into the endogenous *TRA*C locus of CD8 and CD4 T cells (**Figure 2a**). Each neoTCR candidate was then tested for recognition of the cognate neoantigen or mismatched neoantigen controls to confirm neoantigen peptide-HLA specific binding and interferon-gamma (IFNγ) cytokine secretion. This step of confirmation of the reconstituted neoTCR binding to the soluble peptide-HLA complex resulted in 73 out of the 127 tested TCRs (57%) being confirmed as specific and sufficiently

functional neoTCRs for product selection (**Extended Data Table 1**), highlighting the value of testing the candidate neoTCRs before proceeding with the clinical grade manufacturing of the neoTCR gene modified T cell product. Preclinical proof-on-concept data demonstrated that neoTCRs isolated by our approach, when engineered into primary T cells, were able to specifically recognize and kill tumour cells expressing endogenous levels of the neoantigen (**Extended Data Figure 1b** and ref. [20]). Furthermore, to retrospectively benchmark the neoTCRs selected for product generation in our trial, we generated T cells products for seven clinically active TCRs [21-27]. This showed that approximately 50% (18/37) of the neoTCRs we selected have a similar TCR potency as measured by IFNγ production (**Extended Data Figure 1c**).

Up to three confirmed neoTCR candidates per patient were selected for clinical manufacture with a focus on TCR functionality and TCR binding in CD8 and CD4 T cells, diversifying among HLAs and the targeted neoantigens and clonality of the targeted neoantigen (**Extended Data Table 2**). The resulting 37 neoTCRs that were infused into the 16 patients in this clinical trial had IFNγ half maximal effective concentrations (EC_{50}) between 0.4 pg/ml for the highest affinity TCR, to 362 pg/ml for the lowest affinity TCR. Eighteen of the neoTCRs (48%) had an EC_{50} greater than 30 pg/ml, eleven (30%) had an EC_{50} between 30 and 3 pg/ml and were considered good affinity TCRs, while eight (22%) had an EC_{50} lower than 3 pg/ml and were considered high affinity TCRs (**Extended Data Table 2**). The full length TCR sequences, HLA alleles, and neoepitope sequences for the 37 TCRs are available in **Supplementary Table 2**.

Non-viral precision TCR replacement

Patients with relapsed or refractory metastatic solid tumours who had progressed on standard of care treatment options for their cancer, with adequate performance status, evidence of measurable disease, and fulfilling eligibility criteria were considered for leukapheresis when up to three neoTCRs had been selected by the personalized prediction and isolation of neoTCR from

their PBMCs and tumour biopsies. Patients underwent leukapheresis at their local institution, and the leukapheresis product was shipped to the sponsor for manufacturing. CD4 and CD8 T cells were isolated using automated magnetic separation cell sorting and activated for two days, after which cells were electroporated for introduction of the Cas9 protein, guide RNAs to knock-out the endogenous *TRAC* and *TRBC* genes, and an HR template plasmid encoding the transgenic neoTCR. T cells were placed back in culture for expansion for 11 days and the final cell product was cryopreserved on day 13 for infusion on a flexible schedule (**Figure 1a**).

The single-step precision genome engineering results in the seamless replacement of the endogenous TCR with the patient's native sequence neoTCR, whose expression was placed under endogenous promoter regulation (**Figure 2a**). Infused CD8 and CD4 T cells expressing the neoTCRs were detected by flow cytometric analysis using the cognate fluorescently labelled peptide-HLA multimer and ranged from 1.9 to 46.8% of the live cell product (**Extended Data Table 2**). The remaining cell product consisted of T cells that had knock-out of the endogenous TCR, but no knock-in of the neoTCR (KO), or wild-type T cells still expressing the endogenous TCR (WT). Relative neoTCR affinity was determined by the ability of cognate peptide-HLA multimer to bind the neoTCR expressed by CD8 or CD4 T cells. Higher affinity neoTCRs can bind the peptide-HLA target in the absence of the CD8 co-receptor, whilst lower affinity TCRs need CD8 co-receptor stabilization. Based on this, TCRs can be classified as CD8-dependent or -independent binders (**Figure 2b**). Both CD8 and CD4 T cells showed insertion of the transgenes, detected by intracellular staining for the 2A peptide that separates the neoTCR alpha and beta chains (**Figure 2b, Extended Data Figure 1d)**. Assessment of clinical cell products by targeted locus amplification (TLA) confirmed on-target integration of the transgenic TCR cassette (**Extended Data Figure 1e**). Analysis by fluorescence *in situ* hybridization (FISH) indicated a slight increase (P value = 0.0137) in chromosomal aberrations at the chromosome 7 and 14 target sites (**Extended Data Figure 1f**), suggesting the presence of *TRAC:TRBC* translocations.

However, cells harbouring translocations, including cells with *TRAC:TRBC* translocations, were found by others to not exhibit a growth advantage and the frequency of these translocations decreased over time [28,29].

The potency of the final cell product was assessed by measuring IFNγ secretion by ELISA from neoTCR gene edited T cells exposed to the cognate peptide-HLA multimer and was highly correlated (Pearson r = 0.8412, p<0.0001), with the IFNγ response measured by cytokine bead array (CBA) of the same neoTCR in healthy donor cells generated at small-scale for initial product selection (**Figure 2c**), further validating the neoTCR product selection process. In addition to IFNγ secretion, cells displayed a polyfunctional cytokine secretion profile in response to mutational neoantigen peptide-HLA complexes, expressing CD107a on the cell surface and producing TNFα and IL-2 (**Extended Data Figure 2a**). NeoTCR T cells proliferated in a dose-dependent manner in response to neoantigen peptide-HLA stimulation (**Figure 2d** and **Extended Data Figure 2b-c**). Wild type cells (defined as having no evidence of CRISPR knock-out or knock-in of the TCR) proliferated in response to the positive control T cell stimulation using anti-CD3/CD28, but not with the cognate neoantigen peptide-HLA complexes. *TRAC* and *TRBC* knock-out cells do not have a TCR complexed with CD3 chains on their surface and did not proliferate in response to stimulation with either the anti-CD3/CD28 positive control stimulation or with cognate neoantigen peptide-HLA specific stimulation. Additional characterization revealed that the T cell phenotype shifted from a predominantly T cell effector-like (Teff) phenotype in the incoming leukapheresis product to a predominantly T memory stem cell (Tmsc) and T central memory (Tcm) phenotype for each neoTCR cell product lot (**Extended Data Figure 3a**). There was infrequent expression of the costimulatory and coinhibitory surface markers 4-1BB/CD137, LAG-3 or PD-1 (**Extended Data Figure 3b**). There was frequent expression of TIM-3, which has been previously related to the presence of gamma-chain cytokines in the cell culture [30]. CD73 and CD39, which are

upregulated on T cells during activation and differentiation [31], were also expressed by the manufactured cell product.

During the course of the clinical trial, the medium formulation was changed to improve cell growth and editing efficiency of the clinical-grade preparations (cell manufacture versions 2.0 to 2.1), and we also changed the electroporation device (cell manufacture versions 2.1 to 3, **Supplementary Table 3**). The change impacted the quality and quantity of the clinical-grade preparations, with an increase in the neoTCR knock-in from 13.4% to 23.0% (range 1.9-28.3% and 11.4-46.8% for cell manufacture versions 2.0 and 2.1, respectively) and increases in the total numbers of neoTCR-transgenic T cells manufactured (1.08×10^9 to 1.78×10^9). The switch in electroporation devices improved the gene editing efficiencies resulting in robust knock-in and better knock-out reducing the WT population in the final product to less than 10% (**Extended Data Table 2, Extended Data Figure 3c-d**).

Patient enrolment and treatment delivery

From December of 2019 to August of 2022, the study was active at 9 investigational sites. One-hundred-eighty-seven patients signed the informed consent to initiate the process of personalized neoTCR discovery. After successfully obtaining the appropriate quality of baseline biopsies and PBMC for DNA and RNA sequencing, 88 patients (47%) entered the neoTCR discovery process and 46 patients (52%) of these patients met the requirements for successful product selection for clinical manufacture (**Figure 3a**). Twenty-eight patients underwent apheresis and data from 16 patients dosed with neoTCR-transgenic T cell products generated using the V2.0, V2.1 or V3.0 manufacturing process have been included here. Patients had a median age of 47 years (range 36-70) and had received a median of 5 prior lines of therapy (range 2-9) at the time of consent. Patients with cancer histologies across the tumour-mutation burden spectrum were enrolled, and the infused cohort included 11 patients with microsatellite stable-colorectal cancer, two with

hormone receptor positive breast cancer, and one each with ovarian cancer, melanoma and lung cancer (**Extended Data Table 3**). Patients received a total of 4×10^8 (dose level 1), 1.3×10^9 (dose level 2), or 4×10^9 (dose level 3) neoTCR-transgenic T cells within three cell dose cohorts, with four additional patients at the first two dose levels receiving subcutaneous IL-2 post-infusion, which per protocol could be added to the regimen once at least three patients had been dosed at that dose cohort and cleared its safety. Nine patients received cell products with three neoTCRs, three with two neoTCRs, and four with one neoTCR each. The four patients in dose level 1 received a lymphodepleting conditioning regimen of 300 mg/m^2 of cyclophosphamide and 30 mg/m^2 of fludarabine for three days, which led to suboptimal depletion based on the absolute lymphocyte counts. The regimen was modified for the remainder of the study and increased to 600 mg/m^2 of cyclophosphamide for three days and 30 mg/m^2 of fludarabine for four days (**Extended Data Table 3** and **Extended Data Figure 4a**). A step-by-step timeline from TCR discovery and validation through product release for each patient is shown in **Extended Data Figure 4b**. Screening through TCR discovery took a median of 167 days, which included the steps of informed consent through a sequenced biopsy accepted for pipeline analysis (60 days), bioinformatics (11 days), neoantigen peptide-HLA complex isolation (62 days), neoTCR functional characterization in healthy donor T cells (29 days), and product selection of the neoTCRs for dosing (5 days). After selection of the neoTCRs, patients were eligible for enrolment, with a median of 102 days between enrolment and dosing. This included plasmid manufacturing (median 11 days), neoTCR transgenic T cell manufacturing (13 days), and lot release testing (28 days). This period also included additional time before apheresis was scheduled (32 days). Once a product passed lot release, there was a median of 18 days before the patient was dosed.

Infused neoTCR-engineered T cells in patients

We performed repeated peripheral blood sampling from patients to study the engraftment and expansion of the neoTCR-transgenic cells post-infusion over time. The peak of total neoTCR-

transgenic T cells detected in patient's blood increased with the increase in cell dose, occurring at a median time of 2 days post-infusion (range 1-15 days) for the 16 patients dosed, and the percent of neoTCR+ cells in in the infused product correlated with the pharmacokinetic area under the curve through day 7 (**Figure 3b, Extended Data Figure 4c-d**). In dose level 1, with the original lymphodepleting regimen, the median peak of neoTCR-transgenic cells was 1.9% (range 0.9 to 3.3%), which increased to a median of 10.0% (range 7.7 to 12.1%) and 15.0% (range 12.0 to 37.7%) in dose levels 2 and 3, respectively, in patients who received the modified conditioning chemotherapy regimen. With the original conditioning chemotherapy regimen, patients had absolute lymphocyte counts less than 100 cells/μL for a median of 1.5 days (range 0 to 3), which increased to a median of 4 days (range 1 to 10) with the modified conditioning regimen (**Extended Data Figure 4a**). The addition of subcutaneous IL-2 resulted in a peak of neoTCR-transgenic T cells of 7.3% and 6.3% in two patients in dose level 1 (0604, and 0411, respectively). Patient 0026 was treated IL-2 in dose level 2, using version 2.0 of the cell manufacturing process, and had a peak of 9.5% neoTCR-transgenic T cells. The two patients who received cell products generated by version 3.0 manufacturing had the highest levels of circulating neoTCR-transgenic T cells, peaking at 20.8% for patient 1003 in dose level 2 with the addition of subcutaneous IL-2, and at 37.3% for patient 0417 in dose level 3. Overall, strengthening the conditioning chemotherapy, adding IL-2, and increasing neoTCR positive cells while decreasing WT cells in the final cell product each may contribute to improving the maximum concentration and prolonging the exposure of neoTCR T cells detected in the peripheral blood (**Figure 3b, Extended Data Figure 4a, c-d**).

One role of the lymphodepleting conditioning regimen is to increase the availability of the T cell homeostatic expansion cytokines IL-7 and IL-15 in serum, favouring the expansion of the infused T cells [14]. Increased IL-7 and IL-15 levels were observed in serum from patients in the clinical trial, with peak concentrations primarily observed at the time of infusion (**Extended Data Figure**

5a). Analysis of other circulating cytokines demonstrated early peak increases in IFNγ, TNFα, IL-6, IL-8, and IL-10 in occasional patients, with no clear relation with toxicities and at levels that were much lower than serum levels of these cytokines in cases with CRS in other clinical trials [32,33]. Circulating IL-2 could only be detected in the patients who received supplemental subcutaneous IL-2 dosing (**Extended Data Figure 5a**).

NeoTCR-transgenic T cells recovered from blood post-infusion, generally maintained the phenotypes of the infusion product, with Tmsc and Teff being the predominant phenotypes (**Extended Data Figure 5b**). There were infrequent increases in the surface expression of CD73, LAG-3, and PD-1, while CD137/4-1BB remained low (**Extended Data Figure 5c**). Expression of TIM-3 and CD39 decreased in the neoTCR-transgenic cells recovered from patients post-infusion as compared to pre-infusion, further suggesting that their expression in the infusion product was due to the day 2 activation and the presence of exogenous cytokines during the manufacturing process [30].

neoTCR T cells in post-treatment tumour biopsies

In addition to the screening biopsy for neoantigen prediction and identification, patients provided a baseline biopsy (day 5-7 prior to lymphodepletion) to assess continued neoantigen gene expression, and a post-infusion biopsy (day 5-7 or 28) to analyse for neoTCR-transgenic T cell infiltration. Of the eight patients with longitudinal biopsies available for analysis, 15 of 21 predicted truncal neoantigen targets were detected at screening and baseline biopsies (**Extended Data Figure 6a**). Patient 0010 was the only patient whose targeted mutations were not detected in the longitudinal baseline or post-infusion biopsies (n=3), explained by this patient's cancer demonstrating a very strong APOBEC somatic mutation signature (retrospective analysis, **Extended Data Figure 6b**), which has previously been reported to drive extreme tumour heterogeneity [34]. Patient 0605 had a neoTCR targeting a neoepitope predicted to be a sub-clonal

mutation in GPSM2, which was absent in follow-up biopsies. Patient 0506 had a neoepitope mutation in PREP that was undetectable in longitudinal tumour biopsies but was detectable by a bespoke ctDNA assay at both subsequent time points (**Extended Data Figure 6c**), suggesting that ctDNA may be complimentary to tissue biopsies for accurately identifying sub-clonal mutations. In addition, we performed retrospective HLA loss of heterozygosity (LOH) analysis on biopsy samples from infused patients. Analysis showed that LOH of the specific HLA allele presenting a selected neoantigen epitope had occurred prior to treatment in three patients affecting four of the 37 TCRs that were selected and infused (**Extended Data Figure 7a)**. Hence, a subset of the neoantigen mutations presented by specific HLA alleles that had been targeted by the dosed neoTCRs were not presented at the time of infusion. This demonstrates both the importance of HLA LOH analysis for TCR-T cell therapies, as well as the value of identifying sets of therapeutic TCRs that are not limited by specificity against neoantigens presented by a single HLA allele.

Sequence quantification of the TCR complementary-determining region 3 (CDR3) was performed on tumour biopsies before and after infusion (**Figure 4a and b** and **Extended Data Figure 7b**). The genetically introduced neoTCRs frequently were among the top represented TCR CDR3 sequences in these biopsies, with 12 of the infused neoTCR sequences being among the top 4% CDR3 sequences found in post-infusion biopsies, six of which were from patients at dose level 3 (**Figure 4b, Extended Data Figure 7b)**. Immediately flanking the CDR3 sequence is a short codon optimized constant region that can serve as a barcode to differentiate between the native neoTCR and the transgenic neoTCR CDR3 sequences (**Extended Data Figure 7c**). This allowed us to distinguish the neoantigen-specific native T cells from neoTCR-transgenic T cells, and to quantify the infiltration of neoTCR-transgenic T cells into tumours post-infusion. By this approach, 22 separate populations of infused neoTCR-transgenic T cells were detected in the tumours.

Interestingly, only two of 22 populations (TCR913 and TCR441) of neoantigen-specific native T cells were evident in pre-infusion tumour biopsies. TCR441 was found at a very high frequency in the blood at time of product selection for patient 0010 (145 per 168,000 CD8 cells, **Figure 1b**), constituting 0.09% of CD8+ T cells in the blood. In both the baseline and post-infusion biopsies, the TCR441 barcode could not be detected directly although the native sequence could, suggesting the presence of native but not transgenic TCR441. TCR913 (from patient 0612) was detected in the pre-infusion and post-infusion biopsies, and the detection of the TCR913 barcode in the post-infusion biopsy suggests the presence of the infused TCR913-transgenic T cells. TCRs with a lower IFNγ EC_{50} or higher affinity score (a measure of CD8 independent binding) were more likely to be found in the tumour, with 16 of 22 individual T cell populations detected in the analysed post-infusion biopsies from the eight patients with biopsies available for analyses (**Extended data Figure 7 d,** * $p<0.05$). For patient 0503 infused with a three neoTCR product, the presence of the neoTCRs were inferred by the flanking barcode sequence (**Figure 4a** and **b**) but the CDR3 sequence for the specific neoTCR could not be resolved.

The presence of neoTCR-transgenic T cells in the post-infusion biopsies was additionally confirmed by fluorescence microscopy using RNAscope *in situ* hybridization (ISH) probes that were developed to specifically detect the mRNA sequences of the neoTCR knock-in construct. Using this approach for four of the post-dosing biopsies, we directly visualized the intra-tumoural presence of the neoTCR-transgenic cells, frequently in physical contact with cancer cells (**Figure 4c**), demonstrating that the infused neoTCR-transgenic T cells trafficked to solid tumour metastases. The neoTCR-transgenic cell frequency determined from these images showed good correlation with the neoTCR transgene sequencing read counts (Pearson coefficient of 0.8, **Extended Data Figure 7e**).

Toxicities, response and patient outcomes

All patients experienced grade 3-4 pancytopenia, which is an expected toxicity due to the lymphodepletion conditioning regimen. There were two events of a toxicity possibly attributed to the neoTCR-transgenic T cell therapy: one patient (0613) with a grade 1 cytokine release syndrome (CRS), which occurred in the setting of febrile neutropenia; and one patient (1003) with grade 3 encephalitis presenting as difficulty walking, tremulous, difficulty writing on day 7 post-infusion, which was treated with high dose corticosteroids for four days with resolution of symptoms (**Extended Data Table 3**). Eleven patients had disease progression and five patients had stable disease as their best response at their first tumour assessment (day 28 post-infusion, **Extended Data Table 3** and **Extended Data Figure 7f**). Two of these patients had decreases in size of some of the target lesions. This included the first patient in the clinical trial, 0010 in dose level 1, who had a 17% decrease in size of the sum of maximum diameter of target lesions on day 28. This patient had metastatic breast cancer and had received seven prior lines of therapy, but it could be argued that this cancer may have responded to high doses of cyclophosphamide from the preconditioning regimen. Since there was limited *in vivo* expansion of the infused neoTCR-transgenic T cells in patient 0010, an APOBEC signature with loss of the targeted neoantigens and HLA-LOH for one of the targeted alleles was detected retrospectively, the decrease in size of target lesions may be due to the conditioning chemotherapy. Patient 1003, the last patient in the clinical trial, had a metastatic non-small cell lung cancer with six prior lines of therapy (three at consent and three more prior to neoTCR transgenic T cell infusion). This patient had stable disease on day 28 scans with an overall sum of target lesions of -2% from baseline scans, with decrease in size in target lesions in the liver, lymph nodes and ovary (**Extended Data Figure 7g**), and concomitant increase in size in metastatic lesions at other metastatic sites. While no post-treatment biopsy samples were available to look for T cell infiltration or detection of the targeted neoantigens, the high percentage of neoTCR transgenic T cells detected in the periphery and the decrease in some, but not all target lesions could suggest some effect of the therapy.

Discussion

Here we developed and utilized a confluence of technologies to efficiently define the landscape of T cell responses to mutational neoantigens presented by over 60 HLA class I alleles, to clone neoTCR genes from individual T cells and, finally, to genetically engineer them back into autologous T cells using non-viral gene editing techniques. In doing so, we demonstrate that it is realistic to generate personalized T cell therapies with neoantigen-specific TCRs for ACT. When infused into patients, these neoTCR-transgenic T cells circulate through the blood and were detected in tumour metastases at frequencies higher than baseline native T cells with the same neoantigen-specific TCRs.

The technology described herein demonstrates the feasibility and safety of non-viral precision genome engineering for the manufacturing of clinical grade gene-engineered ACT products. A similar approach has been recently used to insert a CD19 chimeric antigen receptor (CAR) into the *PD-1* locus and infused to patients with B cell non-Hodgkin lymphomas with high level of antitumor activity [35]. The use of an HR template plasmid instead of a virus for the delivery of the inserted payload allows for rapid and personalized vector generation used in both, the prototype testing of neoTCR candidates as well as the generation of good manufacturing practices (GMP)-grade plasmid material for clinical-grade cell manufacturing. Using this strategy, we have overcome the hurdles of lengthy and expensive generation of virus-based vectors for introduction of the genetic payload, which hampers their use for personalized ACT. The cloning and GMP manufacturing of the HR template plasmid is rapid and cost-effective, and the precision targeted integration in the T cell genome affords an extra level of safety compared to random integration associated with viral vectors. A further advantage is the ability to integrate payloads exceeding the packaging limits of adeno-associated viruses and other viral vectors.

The clinical trial approach described herein has several limitations. A major limitation of an approach targeting personalized neoantigens is the limited ability and time to characterize each of them for protein expression and neoepitope presentation. Here we used an assessment of the gene expression as well as mutation truncality for the selection of neoantigens being targeted. Favouring mutations induced by oncogenic events in the first cancer clone (for example, from carcinogens like tobacco or ultraviolet light) should result in truncal mutations, as opposed to targeting mutations induced by DNA repair syndromes or APOBEC, with higher likelihood for divergent heterogeneous evolution [36]. We have thought to target truncal mutation wherever possible, however truncality determinations from a single biopsy are not perfect and additional samples, e.g. in form of ctDNA are desirable. Additionally, retrospective analysis of the screening biopsies demonstrated that four of the selected neoTCRs were restricted by an HLA exhibiting LOH, highlighting that LOH analysis should be included in the screening protocol before deciding which neoantigens to target [37]. Given the potential for immunoediting of highly immunogenic neoantigens, baseline biopsies should be analysed for the status of antigen presenting machinery molecules to rule out LOH of *HLA* alleles, and alterations in *TAP* transporters or *B2M* [38-40].

Another complexity of the personalized approach results from the different affinities of the neoTCRs selected for each patient. In the current work, we initially cast a wide net based on literature that suggested that low affinity TCRs T cells could be beneficial in chronic viral infections [41]. To provide a benchmark for TCRs used in adoptive cell therapies for the treatment of solid cancers, we directly compared the activity of neoTCRs used in our clinical trial with prior well-characterized TCRs to shared antigens such as MART-1, Kras-G12D, HPV E6 and E7, mutated P53 or NY ESO-1 for which clinical data were available [21-27]. These TCRs were shown to have EC_{50} activities below 10 ng/mL with the exception of the HPV-E6 TCR, which had an EC_{50} of 63 ng/ml. In comparison, only eight out of 37 TCRs that were selected for the cell products in our neoTCR clinical trial had IFNγ EC_{50} below 10 ng/ml. As we learned from our own data about

449 neoTCR T cell trafficking into the tumor and more clinical data became available [42,43], we tightened
450 the TCR affinity criteria for product selection in favour of higher affinity TCRs, which applied to
451 the last two patients dosed on the current clinical trial (0417 and 1003).
452
453 Lastly, the personalized neoTCR isolation, cloning, validation and selection resulted in a lengthy
454 process, heavily dependent on the quality of the tumour and PBMC samples available for
455 analysis. Time to obtain additional samples and repeated analysis, particularly for screening of
456 TCRs, delayed the ability to infuse the neoTCR cell products to patients. This could be mitigated
457 by streamlined sample acquisition and process automation in the future. A potential solution for
458 both issues with the TCR and neoantigen variability as well as the lengthy product selection
459 process, would be using the same technology for TCR discovery and validation to generate a pre-
460 established library of TCRs specific for common mutations and viral antigens that would cover
461 multiple HLA specificities.
462
463 With the original conditioning chemotherapy, manufacturing (processes V2 and V2.1) and the two
464 low cell dose cohorts, there was very limited *in vivo* expansion of the infused neoTCR gene-edited
465 T cells, which likely resulted in low probability of clinical benefit. The dose escalation study started
466 with cell doses that may be lower than would be needed for the potential of a clinical response,
467 especially if we consider that the total transgenic cell dose was divided by the three TCRs in many
468 patients. In the solid tumor setting, TCR transgenic T cell clinical trials conducted by others have
469 shown clinical activity in the 5-10 x 10^9 per TCR range, with no clear dose response beyond 10
470 billion cells per TCR [42,43]. The improvements in the manufacturing during the conduct of the trial
471 and progressing through the cell doses led to a better *in vivo* expansion in the last patients dosed,
472 getting closer to the levels that would be therapeutic in other studies [21-27].
473

In conclusion, in the current work we demonstrate the ability to use CRISPR-based, non-viral knock-out and knock-in editing to genetically redirect T cells to mutational neoantigens in humans. This work builds on pioneering research of genome editing to redirect T cell specificity with transgenic TCR engineering [44] to generate a widely applicable, tumour-specific, personalized T cell therapy for patients with solid cancers. The substitution of the endogenous TCR with a neoTCR results in T cells that only react to the mutation presented by a specific HLA, providing a safe target for T cell engineering and redirection to cancer cells. With the demonstration of feasibility and safety of this approach, neoTCR-engineered T cells could be further genetically engineered to increase their functionality. The versatility of the non-viral gene editing approach, which in a single-step allows knocking-out and knocking-in of several genes, predicts that near future clinical approaches will be able to incorporate additional gene edits that improve T cell function, avoid T cell exhaustion, permit T cells to continue to react to antigen despite repeated antigen encounters, avoid the immune suppressive factors in the solid tumour microenvironment, and allow *in vivo* expansion even without the need for lymphodepleting conditioning chemotherapy. There are many potential targets resulting from T cell biology studies in the past decades, T cell functional analyses from knock-out mice, recent CRISPR screens, and engineering of synthetic receptors [29,45-49], which will provide a path to generate neoTCR engineered T cell therapies with the ability permit controlled *in vivo* expansion and avoid T cell exhaustion, hopefully resulting in complete and durable responses for patients with solid tumours.

Main Article References

1 Matsushita, H. *et al.* Cancer exome analysis reveals a T-cell-dependent mechanism of cancer immunoediting. *Nature* **482**, 400-404, doi:10.1038/nature10755 (2012).

2 van Rooij, N. *et al.* Tumor Exome Analysis Reveals Neoantigen-Specific T-Cell Reactivity in an Ipilimumab-Responsive Melanoma. *J Clin Oncol*, doi:10.1200/JCO.2012.47.7521 (2013).

3 Schumacher, T. N. & Schreiber, R. D. Neoantigens in cancer immunotherapy. *Science* **348**, 69-74, doi:10.1126/science.aaa4971 (2015).

4 Gros, A. *et al.* Prospective identification of neoantigen-specific lymphocytes in the peripheral blood of melanoma patients. *Nat Med* **22**, 433-438, doi:10.1038/nm.4051 (2016).

5 Tran, E. *et al.* Cancer immunotherapy based on mutation-specific CD4+ T cells in a patient with epithelial cancer. *Science* **344**, 641-645, doi:10.1126/science.1251102 (2014).

6 Sahin, U. *et al.* Personalized RNA mutanome vaccines mobilize poly-specific therapeutic immunity against cancer. *Nature* **547**, 222-226, doi:10.1038/nature23003 (2017).

7 Sahin, U. & Tureci, O. Personalized vaccines for cancer immunotherapy. *Science* **359**, 1355-1360, doi:10.1126/science.aar7112 (2018).

8 Hu, Z. *et al.* Personal neoantigen vaccines induce persistent memory T cell responses and epitope spreading in patients with melanoma. *Nat Med* **27**, 515-525, doi:10.1038/s41591-020-01206-4 (2021).

9 Lowery, F. J. *et al.* Molecular signatures of antitumor neoantigen-reactive T cells from metastatic human cancers. *Science*, eabl5447, doi:10.1126/science.abl5447 (2022).

10 Ott, P. A. *et al.* An immunogenic personal neoantigen vaccine for patients with melanoma. *Nature* **547**, 217-221, doi:10.1038/nature22991 (2017).

11 Robinson, J. *et al.* The IPD and IMGT/HLA database: allele variant databases. *Nucleic Acids Res* **43**, D423-431, doi:10.1093/nar/gku1161 (2015).

12 Greenbaum, U., Dumbrava, E. I., Biter, A. B., Haymaker, C. L. & Hong, D. S. Engineered T-cell Receptor T Cells for Cancer Immunotherapy. *Cancer immunology research* **9**, 1252-1261, doi:10.1158/2326-6066.CIR-21-0269 (2021).

13 Peng, S. *et al.* Sensitive Detection and Analysis of Neoantigen-Specific T Cell Populations from Tumors and Blood. *Cell reports* **28**, 2728-2738 e2727, doi:10.1016/j.celrep.2019.07.106 (2019).

14 Rosenberg, S. A., Restifo, N. P., Yang, J. C., Morgan, R. A. & Dudley, M. E. Adoptive cell transfer: a clinical path to effective cancer immunotherapy. *Nat Rev Cancer* **8**, 299-308, doi:nrc2355 [pii]
10.1038/nrc2355 (2008).

15 Roth, T. L. *et al.* Reprogramming human T cell function and specificity with non-viral genome targeting. *Nature* **559**, 405-409, doi:10.1038/s41586-018-0326-5 (2018).

16 Oh, S. A. *et al.* High-efficiency nonviral CRISPR/Cas9-mediated gene editing of human T cells using plasmid donor DNA. *J Exp Med* **219**, doi:10.1084/jem.20211530 (2022).

17 Eyquem, J. *et al.* Targeting a CAR to the TRAC locus with CRISPR/Cas9 enhances tumour rejection. *Nature* **543**, 113-117, doi:10.1038/nature21405 (2017).

18 Muller, T. R. *et al.* Targeted T cell receptor gene editing provides predictable T cell product function for immunotherapy. *Cell Rep Med* **2**, 100374, doi:10.1016/j.xcrm.2021.100374 (2021).

19 Ruggiero, E. *et al.* CRISPR-based gene disruption and integration of high-avidity, WT1-specific T cell receptors improve antitumor T cell function. *Sci Transl Med* **14**, eabg8027, doi:10.1126/scitranslmed.abg8027 (2022).

20 Puig-Saus, C. *et al.* Landscape analysis of neoepitope-specific T cell responses to immunotherapy. *Proc American Association for Cancer Research* **NextGen Award session** (2020).
21 Johnson, L. A. *et al.* Gene therapy with human and mouse T-cell receptors mediates cancer regression and targets normal tissues expressing cognate antigen. *Blood* **114**, 535-546, doi:blood-2009-03-211714 [pii]
10.1182/blood-2009-03-211714 (2009).
22 Robbins, P. F. *et al.* Tumor regression in patients with metastatic synovial cell sarcoma and melanoma using genetically engineered lymphocytes reactive with NY-ESO-1. *Journal of clinical oncology : official journal of the American Society of Clinical Oncology* **29**, 917-924, doi:10.1200/JCO.2010.32.2537 (2011).
23 Tran, E. *et al.* T-Cell Transfer Therapy Targeting Mutant KRAS in Cancer. *N Engl J Med* **375**, 2255-2262, doi:10.1056/NEJMoa1609279 (2016).
24 Malekzadeh, P. *et al.* Neoantigen screening identifies broad TP53 mutant immunogenicity in patients with epithelial cancers. *J Clin Invest* **129**, 1109-1114, doi:10.1172/JCI123791 (2019).
25 Jin, B. Y. *et al.* Engineered T cells targeting E7 mediate regression of human papillomavirus cancers in a murine model. *JCI insight* **3**, doi:10.1172/jci.insight.99488 (2018).
26 Sanderson, J. P. *et al.* Preclinical evaluation of an affinity-enhanced MAGE-A4-specific T-cell receptor for adoptive T-cell therapy. *Oncoimmunology* **9**, 1682381, doi:10.1080/2162402X.2019.1682381 (2020).
27 Draper, L. M. *et al.* Targeting of HPV-16+ Epithelial Cancer Cells by TCR Gene Engineered T Cells Directed against E6. *Clin Cancer Res* **21**, 4431-4439, doi:10.1158/1078-0432.CCR-14-3341 (2015).
28 Poirot, L. *et al.* Multiplex Genome-Edited T-cell Manufacturing Platform for "Off-the-Shelf" Adoptive T-cell Immunotherapies. *Cancer Res* **75**, 3853-3864, doi:10.1158/0008-5472.CAN-14-3321 (2015).
29 Stadtmauer, E. A. *et al.* CRISPR-engineered T cells in patients with refractory cancer. *Science* **367**, doi:10.1126/science.aba7365 (2020).
30 Mujib, S. *et al.* Antigen-independent induction of Tim-3 expression on human T cells by the common gamma-chain cytokines IL-2, IL-7, IL-15, and IL-21 is associated with proliferation and is dependent on the phosphoinositide 3-kinase pathway. *J Immunol* **188**, 3745-3756, doi:10.4049/jimmunol.1102609 (2012).
31 Shevchenko, I. *et al.* Enhanced expression of CD39 and CD73 on T cells in the regulation of anti-tumor immune responses. *Oncoimmunology* **9**, 1744946, doi:10.1080/2162402X.2020.1744946 (2020).
32 Teachey, D. T. *et al.* Identification of Predictive Biomarkers for Cytokine Release Syndrome after Chimeric Antigen Receptor T-cell Therapy for Acute Lymphoblastic Leukemia. *Cancer Discov* **6**, 664-679, doi:10.1158/2159-8290.CD-16-0040 (2016).
33 Wang, M. *et al.* KTE-X19 CAR T-Cell Therapy in Relapsed or Refractory Mantle-Cell Lymphoma. *N Engl J Med* **382**, 1331-1342, doi:10.1056/NEJMoa1914347 (2020).
34 Venkatesan, S. *et al.* Perspective: APOBEC mutagenesis in drug resistance and immune escape in HIV and cancer evolution. *Ann Oncol* **29**, 563-572, doi:10.1093/annonc/mdy003 (2018).
35 Zhang, J. *et al.* Non-viral, specifically targeted CAR-T cells achieve high safety and efficacy in B-NHL. *Nature* **609**, 369-374, doi:10.1038/s41586-022-05140-y (2022).
36 Swanton, C., McGranahan, N., Starrett, G. J. & Harris, R. S. APOBEC Enzymes: Mutagenic Fuel for Cancer Evolution and Heterogeneity. *Cancer Discov* **5**, 704-712, doi:10.1158/2159-8290.CD-15-0344 (2015).

37 McGranahan, N. *et al.* Allele-Specific HLA Loss and Immune Escape in Lung Cancer Evolution. *Cell* **171**, 1259-1271 e1211, doi:10.1016/j.cell.2017.10.001 (2017).
38 Doran, S. L. *et al.* T-Cell Receptor Gene Therapy for Human Papillomavirus-Associated Epithelial Cancers: A First-in-Human, Phase I/II Study. *J Clin Oncol* **37**, 2759-2768, doi:10.1200/JCO.18.02424 (2019).
39 Nagarsheth, N. B. *et al.* TCR-engineered T cells targeting E7 for patients with metastatic HPV-associated epithelial cancers. *Nat Med* **27**, 419-425, doi:10.1038/s41591-020-01225-1 (2021).
40 Kalbasi, A. & Ribas, A. Tumour-intrinsic resistance to immune checkpoint blockade. *Nat Rev Immunol* **20**, 25-39, doi:10.1038/s41577-019-0218-4 (2020).
41 Schober, K. *et al.* Reverse TCR repertoire evolution toward dominant low-affinity clones during chronic CMV infection. *Nat Immunol* **21**, 434-441, doi:10.1038/s41590-020-0628-2 (2020).
42 Wermke, M. *et al.* Safety and anti-tumor activity of TCR-engineered autologous, PRAME-directed T cells across multiple advanced solid cancers at low doses – clinical update on the ACTengine® IMA203 trial. *Journal of immunotherapy for cancer* (2021).
43 Hong, D. S. *et al.* pdated safety and efficacy from SURPASS, the phase I trial of ADP-A2M4CD8, a next-generation autologous T-cell receptor T-cell therapy, in previously treated patients with unresectable or metastatic tumors. *Annals of Oncology* **33** S331-S355 (2022).
44 Provasi, E. *et al.* Editing T cell specificity towards leukemia by zinc finger nucleases and lentiviral gene transfer. *Nat Med* **18**, 807-815, doi:10.1038/nm.2700 (2012).
45 Fraietta, J. A. *et al.* Disruption of TET2 promotes the therapeutic efficacy of CD19-targeted T cells. *Nature* **558**, 307-312, doi:10.1038/s41586-018-0178-z (2018).
46 Sen, D. R. *et al.* The epigenetic landscape of T cell exhaustion. *Science* **354**, 1165-1169, doi:10.1126/science.aae0491 (2016).
47 Li, M. O., Wan, Y. Y., Sanjabi, S., Robertson, A. K. & Flavell, R. A. Transforming growth factor-beta regulation of immune responses. *Annu Rev Immunol* **24**, 99-146 (2006).
48 Schmidt, R. *et al.* CRISPR activation and interference screens decode stimulation responses in primary human T cells. *Science* **375**, eabj4008, doi:10.1126/science.abj4008 (2022).
49 Kalbasi, A. *et al.* Potentiating adoptive cell therapy using synthetic IL-9 receptors. *Nature* **607**, 360-365, doi:10.1038/s41586-022-04801-2 (2022).

Methods References

50 Li, H. Aligning sequence reads, clone sequences and assembly contigs with BWA-MEM. *arXiv* https://doi.org/10.48550/arXiv.1303.3997 (2013).

51 Koboldt, D. C. *et al.* VarScan 2: somatic mutation and copy number alteration discovery in cancer by exome sequencing. *Genome research* **22**, 568-576, doi:10.1101/gr.129684.111 (2012).

52 Cibulskis, K. *et al.* Sensitive detection of somatic point mutations in impure and heterogeneous cancer samples. *Nat Biotechnol* **31**, 213-219, doi:10.1038/nbt.2514 (2013).

53 Saunders, C. T. *et al.* Strelka: accurate somatic small-variant calling from sequenced tumor-normal sample pairs. *Bioinformatics* **28**, 1811-1817, doi:10.1093/bioinformatics/bts271 (2012).

54 Lai, Z. *et al.* VarDict: a novel and versatile variant caller for next-generation sequencing in cancer research. *Nucleic Acids Res* **44**, e108, doi:10.1093/nar/gkw227 (2016).

55 Dobin, A. & Gingeras, T. R. Mapping RNA-seq Reads with STAR. *Curr Protoc Bioinformatics* **51**, 11 14 11-11 14 19, doi:10.1002/0471250953.bi1114s51 (2015).

56 Szolek, A. *et al.* OptiType: precision HLA typing from next-generation sequencing data. *Bioinformatics* **30**, 3310-3316, doi:10.1093/bioinformatics/btu548 (2014).

57 Reynisson, B., Alvarez, B., Paul, S., Peters, B. & Nielsen, M. NetMHCpan-4.1 and NetMHCIIpan-4.0: improved predictions of MHC antigen presentation by concurrent motif deconvolution and integration of MS MHC eluted ligand data. *Nucleic Acids Res* **48**, W449-W454, doi:10.1093/nar/gkaa379 (2020).

58 Favero, F. *et al.* Sequenza: allele-specific copy number and mutation profiles from tumor sequencing data. *Ann Oncol* **26**, 64-70, doi:10.1093/annonc/mdu479 (2015).

59 Roth, A. *et al.* PyClone: statistical inference of clonal population structure in cancer. *Nat Methods* **11**, 396-398, doi:10.1038/nmeth.2883 (2014).

60 Chang, M. T. *et al.* Accelerating Discovery of Functional Mutant Alleles in Cancer. *Cancer Discov* **8**, 174-183, doi:10.1158/2159-8290.CD-17-0321 (2018).

61 Power, R. P. *et al.* A diagnostic platform for precision cancer therapy enabling composite biomarkers by combining tumor and immune features from an enhanced exome and transcriptome. *Cancer Research* **80**, 1334 (2020).

62 Bolotin, D. A. *et al.* MiXCR: software for comprehensive adaptive immunity profiling. *Nat Methods* **12**, 380-381, doi:10.1038/nmeth.3364 (2015).

63 Diaz-Gay, M. *et al.* Mutational Signatures in Cancer (MuSiCa): a web application to implement mutational signatures analysis in cancer samples. *BMC Bioinformatics* **19**, 224, doi:10.1186/s12859-018-2234-y (2018).

64 Alexandrov, L. B. *et al.* The repertoire of mutational signatures in human cancer. *Nature* **578**, 94-101, doi:10.1038/s41586-020-1943-3 (2020).

65 Smith, C., Ma, Y., Campbell, K. M., Pan, Z. & Stawiski, E. Uncovering HLA loss of heterozygosity in cancer for the improvement of personalized neoTCR immunotherapy with PACT-ESCAPE. *Proc American Association for Cancer Research*, Abstract 1213 (2022).

66 Robinson, J. *et al.* IPD-IMGT/HLA Database. *Nucleic Acids Res* **48**, D948-D955, doi:10.1093/nar/gkz950 (2020).

67 Bratman, S. V. *et al.* Personalized circulating tumor DNA analysis as a predictive biomarker in solid tumor patients treated with pembrolizumab. *Nat Cancer* **1**, 873-881, doi:10.1038/s43018-020-0096-5 (2020).

68 Lybarger, L. *et al.* Enhanced immune presentation of a single-chain major histocompatibility complex class I molecule engineered to optimize linkage of a C-

terminally extended peptide. *J Biol Chem* **278**, 27105-27111, doi:10.1074/jbc.M303716200 (2003).

69 Lefranc, M. P. *et al.* IMGT(R), the international ImMunoGeneTics information system(R) 25 years on. *Nucleic Acids Res* **43**, D413-422, doi:10.1093/nar/gku1056 (2015).

70 Bethune, M. T., Comin-Anduix, B., Hwang Fu, Y. H., Ribas, A. & Baltimore, D. Preparation of peptide-MHC and T-cell receptor dextramers by biotinylated dextran doping. *BioTechniques* **62**, 123-130, doi:10.2144/000114525 (2017).

686 **Figure Legends**

687

688 **Figure 1.** Schematic for TCR discovery through cell manufacturing. **a)** Generation of neoTCR
689 product for each patient is separated into two steps: Screening and Enrolment. Screening begins
690 with identification of patient tumour-specific mutations based on sequencing data and
691 bioinformatic prediction of mutated neoantigen peptides. Native CD8 T cells that bind neoantigen
692 targets are captured from blood using barcoded and fluorescently labelled peptide-HLA
693 multimers. NeoTCR sequences are cloned from captured T cells and functionally characterized
694 in healthy donor T cells before product selection. HR DNA plasmid(s) encoding the selected
695 neoTCR sequence(s) are then manufactured for subsequent cGMP T cell manufacturing. Patients
696 enrol on the study after product selection. Manufacturing begins with apheresis of the patient's
697 blood followed by enrichment of CD8 and CD4 T cells. T cells are *ex vivo* precision genome
698 engineered to express one neoTCR. Cells are expanded, and cryopreserved until the patient is
699 ready for reinfusion. **b and c)** Two examples of neoTCR T cells isolated from patient PBMC. Each
700 box represents one T cell (x = 10 T cells); each colour represents a TCR clone. T cells within
701 dashed boxes target the same peptide-HLA target. Neoepitope amino acid sequence and
702 restricting HLA allele are indicated on top of the boxes. Peptide-HLA targets are indicated by tick
703 marks. Upward x-axis tick indicates peptide-HLA that bound to patient TCR. All T cells shown on
704 graph were a non-naïve phenotype based on CD95 expression. TCRs indicated with numbers
705 and arrows, were selected for clinical scale manufacture **b**) Patient 0010. A total of 262 peptide-
706 HLAs were made. 236 neoantigen-specific T cells were isolated, representing 21 unique
707 neoTCRs. The neoTCRs targeted 8 neoantigens across two HLA's. **c)** Patient 0506. 105 bar-
708 coded peptide-HLAs were made. Six neoantigen-specific T cells were captured representing five
709 unique neoTCRs. The neoTCRs targeted four neoantigens across two HLA's.

710

Figure 2. Non-viral precision genome engineering for clinical grade cell manufacturing. **a)** Schematic of construct design and resulting editing. **b)** Examples of endogenous TCR knock-out and knock-in of up to three neoantigen-specific TCRs (neoTCRs) in clinical final cell product. Day 0 shows an example of the same patient's enriched T cell product but was not stained with the peptide-HLA multimer. Day 13 flow plots show the results of each of the three neoTCR product lots for that patient. CD8 T cells are shown on top and CD4 T cells on the bottom. **c)** TCR functionality as evaluated by IFNγ production correlates between small-scale products generated from healthy donor T cells and large-scale final cell clinical product. Functionality of the neoTCR clinical grade product made for patient autologous cells (IFNγ EC_{50} by ELISA or ELLA Simple Plex) was correlated with functionality of the neoTCR product made in healthy donors at product selection (IFNγ EC_{50} by CBA; Pearson r = 0.8412, p<0.0001). **d)** Proliferation analysis of neoTCR clinical final cell products upon exposure to peptide-HLA stimulation at 1,000 ng/ml. Each dot represents a unique neoTCR product. WT = wild-type, unedited cells expressing the endogenous TCR. NeoTCR+ or GE = Gene Edited: knock-out of wild-type TCR and knock-in of neoTCR. KO = Knock-out of the endogenous TCR only, these cells do not have a TCR on their surface.

Figure 3. Clinical trial patients and samples, and analysis of neoTCR-transgenic T cells in blood post-infusion. **a)** CONSORT diagram with the number of consented patients, patients who went onto TCR isolation, leukapheresis, clinical product manufacturing, infused with neoTCR-transgenic T cells and with blood and biopsy samples for analyses. **b)** Expansion and persistence of neoTCR-transgenic T cells in peripheral blood of patients measured by flow cytometry of peptide-HLA multimer stained cells. Percentages of total T cells from patients in dose level 1 (DL1, left), DL2 (centre), and DL3 (right) are shown. Patients treated with IL-2 combination therapy are indicated by dotted lines. Cancer type is shown next to patient number: breast (BrCa), ovarian, melanoma, colorectal (CRC). All available timepoints were analysed. Patient 0613: 1.3% NeoTCR+ cells at day 106 post-infusion. Limit of detection is approximately 0.16%.

737

738 **Figure 4.** Trafficking of neoantigen-specific TCR (neoTCR) transgenic T cells as detected in
739 tumour biopsies. **a)** Analysis of all available baseline (Pre) and post-infusion (Post) biopsies for
740 the presence of infused neoTCRs from detected CDR3 alpha and barcoded reads for dose level
741 1, 2 and 3 with (+IL2) or without IL2. Colours of boxes indicate cancer type and one TCR for which
742 the sequencing reads supporting the codon optimized constant region was not detected is marked
743 with an orange line (patient 0010). **b)** Quantitation of TCR CDR3 alpha reads in post-infusion
744 biopsies from patients. Dots are labelled both by size (larger if neoTCR barcode was confirmed)
745 and colour. Coloured dots are CDR3 sequences matching neoTCRs, and grey dots are neoTCR
746 unrelated CDR3 alpha reads and their relative quantification. Boxes indicate the interquartile
747 range (IQR); centre line, median; whiskers, lowest and highest values within 1.5x IQR from the
748 first and third quartiles, respectively. **c)** Spatial profiling to image neoTCR-transgenic T cells in
749 tumours. Gray = nuclei, green = neoTCR, magenta = CD3. White arrows denote neoTCR T cells.
750 Scale bar is 20 micrometres.

751

Online Methods

Clinical trial design

This phase 1a trial was a multicentre 3+3 dose escalation study. The primary objectives were to evaluate safety and tolerability, determine a maximum tolerated dose, and evaluate manufacturing feasibility (NCT03970382). Safety and feasibility were assessed for the infusion of up to three distinct neoTCR T cell products for each patient. Patients were treated with neoTCR T cells at doses of 4×10^8 (dose level 1, 1.3×10^8 – 4×10^8 cells/TCR), 1.3×10^9 (dose level 2, 400×10^8 – 1.3×10^9 cells/TCR), and 4×10^9 (dose level 3, 1.3×10^9 – 4×10^9 cells/TCR) neoTCR positive T cells. The total number of gene-edited cells at a given dose level remained the same, regardless of the number of neoTCR T cell products infused (1, 2, or 3). Only participants who received three neoTCR products contributed to clearing a dose level. The first four patients received a conditioning regimen of 30 mg/m^2 fludarabine and 300 mg/m^2 cyclophosphamide intravenously (i.v.; days -5 through -3; 3 doses each) and it was modified to 30 mg/m^2 fludarabine (i.v.; days -6 through -3; 4 doses) and 600 mg/m^2 cyclophosphamide (i.v.; days -5 through -3; 3 doses) for subsequent patients. NeoTCR T cells were infused on day 0, with consecutive infusion of up to three neoTCR T cell products. After safety was evaluated at each dose level, additional participants were eligible for expansion at the cleared dose level along with 500,000 IU/m^2 low-dose IL-2 (aldesleukin) administered subcutaneously (s.c.) twice a day from days 1-7 starting on day 1.

Study Oversight

The protocol was approved by the institutional review board at each site enrolling patients: City of Hope, Duarte California; University of California Los Angeles, Los Angeles California; University of California, Irvine Medical Center, Orange, California; University of California, Davis, Sacramento California; University of California, San Francisco, San Francisco California;

Northwestern University Medical Center, Chicago Illinois; Memorial Sloan Kettering Cancer Center, New York, New York; Tennessee Oncology, Nashville, Tennessee; and Fred Hutchinson Cancer Research Center, Seattle, Washington.. The trial was conducted in accordance with the principles of the Declaration of Helsinki. An independent data and safety monitoring committee regularly reviewed safety data. All patients provided informed written consent. The trial protocol and statistical analysis plan were designed in a collaboration between the sponsor (PACT Pharma Inc.) and the authors.

Patients

Patients were eligible for screening to identify TCRs if they were ≥ 18 years of age, had one of the following metastatic solid tumour types: urothelial carcinoma, melanoma, non-small cell lung carcinoma, head and neck squamous cell carcinoma, colorectal cancer, ovarian cancer, hormone receptor positive and triple negative breast cancer, or prostate cancer, had disease progression after at least one available standard therapy with no additional curative options available, and measurable disease per RECIST v.1.1. Inclusion criteria for TCR identification included providing a tumour biopsy (fresh or archival tumour biopsy within one year of consent) for sequencing and neoantigen prediction, PBMCs for T cell isolation, and a willingness and ability to undergo leukapheresis for cell product manufacture. To decrease the risk of decline during TCR product selection and cell therapy manufacture and infusion, patients were required to have a life expectancy of > 6 months, ECOG of 0 or 1, and adequate hematologic and organ function.

Between consent and neoTCR product selection, patients were able to be treated with anti-cancer therapies. Patients were required to discontinue therapy within two weeks or five half-lives (whichever was shorter) prior to leukapheresis. On successful neoTCR product selection and prior to leukapheresis, patients were required to meet the initial screening criteria with adequate hematologic and organ function. Patients with asymptomatic brain metastasis were included.

Eligible patients had an absolute lymphocyte count of at least 500 cells per cubic millimetre. During manufacturing, patients could receive bridging therapy at the investigator's discretion, after which repeat baseline imaging was performed. Prior to receiving conditioning chemotherapy and cell infusion, patients were required to have no significant changes in status compared to the initial eligibility criteria.

Safety and response assessments

Incidence and nature of adverse events to define dose-limiting toxicities (DLTs) was documented using the NCI CTCAE v5.0 except for CRS and neurotoxicity, which were evaluated per the ASTCT consensus criteria. The DLT assessment window was from day 0 to day 28. A Safety Review Team (SRT) was chartered to review safety after each dose level and prior to opening the IL-2 cohorts. Response assessment for overall response rate (ORR) was determined by investigator assessment using RECIST v1.1 on day 28 and confirmed by repeat assessment ≥4 weeks after initial documentation.

Biospecimen collection and processing

Archival or fresh tumour biopsy specimens were formalin-fixed and paraffin-embedded (FFPE). Paraffin-embedding was performed at the study site or CellCarta (Quebec, Canada). Tumour sectioning was performed by CellCarta and cut sections were used for sequencing at Personalis (Menlo Park, CA) or fluorescence microscopy. Screening peripheral blood samples for sequencing were collected in K2EDTA tubes, processed at Precision for Medicine (Bethesda, MD), and sequenced at Personalis. Peripheral blood samples for T cell identification at screening or on-treatment analysis were collected in ACD or CPT tubes and shipped to Precision for Medicine for PBMC isolation and cryopreservation. For clinical cell product manufacture, a whole leukapheresis product was obtained from the patient at the study site and shipped overnight to

the study sponsor. Samples from each infusion cell product and final clinical cell manufacture product were cryopreserved. Serum and plasma were collected and cryopreserved until analysis.

Neoantigen prediction and truncality estimation

Patient's tumour biopsies and the matched normal sample from PBMC were sequenced to identify expressed non-synonymous coding mutations (NSM). Although most of the analysis was the same, there were 3 versions of the pipeline used throughout the clinical trial and the differences are described below. Samples 0010, 0026, 0503, 0506, 0603, 0604, 0605, 0612 and 0613 were processed on version 1, version 2 processed 0030, 0038, 0404, 0411, and 0611, version 3 processed 0417 and 1003. Briefly, whole exome sequencing (WES) and RNA-Seq from a recent tumour sample in FFPE and PBMC were performed using Illumina HiSeq 2500 platform or NovaSeq 6000 platform (Illumina, San Diego, CA). First, WES sequences were aligned to the human reference genome build 37 (GRCh37/hg19) using BWA-MEM [50]. NSM identified by at least two mutation callers among VarScan2 and MuTect or MuTect2/VarDictJava/Strelka2 were retained as potential neoantigens [51-54]. RNA-Seq sequences were mapped to human genome, quantified and normalized using STAR/RSEM [55]. A minimum of 1 RNA-Seq read was used for conformation of expression, however TPM and expression values were further considered at time of product selection. Next, the neoantigen sequences and patient's HLA types identified from patient's PBMC WES using OptiType [56] were used as input for HLA-peptide binding affinity prediction with netMHCpan. In version 3 of the software, OptiType alignment with RNA-Seq reads to individual restricting HLA's to access expression levels were routinely reported. Version 1 used netMHCpan 3.0, version 2 used netMHCpan4.0 and version 3 used version netMHCpan4.1 [57]. In addition, the truncality and cancer cellular fraction of the detected NSM was predicted based on WES results and was available at time of product selection with preference given to truncal NSMs. Briefly, the read alignment files from WES of tumour biopsies and matched PBMC generated previously were used as input for copy number segmentation, ploidy and tumour purity estimation,

and allelic copy number profiling using Sequenza [58], followed by PyClone analysis as previously described for NSM truncality estimation [59]. Finally, the HLA-peptide complexes with predicted binding affinities among top 2% ranking with respect to each HLA were selected and only the peptides with confirmed expression by RNA-Seq were allowed. A maximum of 352 selections were made per patient. In version 3 of the software, the first 5 epitopes chosen consisted of recurrent driver mutations [60] regardless of ranking if they were present and expressed. Prioritized HLA-peptide complexes were proceeded to protein reagent generation. Neoepitopes that were derived from recurrent driver mutations were noted at time of product selection.

Retrospective sequence analysis of post-dosing and screening samples

Amplicon sequencing-based TCR assays were conducted at Personalis to further interrogate the immune repertoire in tumour biopsies and the CDR3 reads and frequency from TCRα and TCRβ were reported to evaluate the neoTCR trafficking after dosing [61]. To further ensure the integration of neoTCR and its expression in the post infusion biopsies, the tumour sequencing reads from whole-exome sequencing and RNA-Seq were aligned to the gene-editing payload containing neoTCR TCRβ, TCRα, P2A and partial *TRAC* chain following the similar protocols described in the main text. The tumour sequencing reads from RNA-Seq were used as input to the MiXCR program [62]. The TCRα and TCRβ CDR3 sequences in tumour biopsy were identified and compared to neoTCR CDR3 sequences. Five distinct base changes in a short stretch of a codon optimized constant region served as an effective barcode for identifying specific neoTCRs. The sample somatic mutational signatures for patients was determined using MuSiCa from screening WES data [63]. This program compares somatic signature profiles to previously published COSMIC somatic signatures (https://cancer.sanger.ac.uk/signatures/) [64].

HLA LOH was analysed using both WES and RNA-seq data [65] using two complimentary approaches. First, WES data was used to access allelic copy number at HLA loci using Sequenza

[58], with a copy number state of zero denoting putative LOH. To determine which HLA allele was lost, SNP frequencies between alleles were compared with a binomial GLM and the allele with lower SNP frequency assigned to the lower copy number state. Unique SNPs for HLA alleles were derived from IMGT 3.40.3 [66]. Second, allelic imbalance at 26 HLA loci was calculated in DNA and RNA, where allelic imbalance is the normalized ratio of sequencing depth at SNP positions between alleles at a locus. Higher allelic imbalance in DNA corresponds to a greater difference in copy number between alleles, while higher allelic imbalance values in RNA represent a greater difference in the expression of one allele relative to the other. Samples with LOH are expected to have higher allelic imbalance in DNA and RNA because LOH reduces the sequencing depth at SNP positions for the lost allele. Allelic copy number and allelic imbalance in DNA and RNA were then manually reviewed to confirm the HLA LOH classification.

Somatic variants from WES data were used for a custom ctDNA assay made by Natera Inc. (San Carlos, USA) as previously described [67]. Briefly, this assay designs multiplex PCR primers for 16 truncal variants and up-to 16 custom variants of interest. Plasma from longitudinal samples had cfDNA isolated and amplified and subsequently sequenced on an Illumina sequencer. All ctDNA timepoints were normalized by quantifying the mean tumour molecules (MTM) per mL of plasma.

Peptide-HLA protein synthesis

Peptide-HLA complex libraries were generated by assembling single-chain trimers [68], where neoantigen peptides were fused in sequence to beta-2-microglobulin (β2M) domains and the HLA, each domain being linked with $(G4S)_4$ motifs. Briefly, double stranded oligo nucleotides (IDT) were ligated into pcDNA vectors encoding linkers, β2M and the corresponding HLA, and the expression sequence amplified by PCR. Linear amplicons were transfected into Expi293F cells (ThermoFisher, Waltham, MA) following the manufacturers recommendations. Cells were harvested after five days, and supernatants were clarified using 96-well Pall filters. Proteins were

biotinylated with Biotin Ligase BirA (Avidity, Aurora, CO) for two hours at room temperature. Biotinylated proteins were purified by IMAC (Ni-sepharose) using the Phynexus Phytip system and buffer exchanged into HBS using the ThermoFisher Zeba Spin 7k MWCO plates or by Zn(+)-loaded HiTrap capto-chelate resin in tandem with HiTrap Desalting columns to remove imidazole. Protein concentration was determined by absorbance at 280 nm.

NeoTCR isolation

Each purified patient peptide-HLA protein was multimerized, fluorescently labelled, and DNA barcoded. The barcode followed the structure Adaptor-UMI-Barcode-UMI-Adaptor (Integrated DNA Technologies, Coralville, IA). Briefly, biotinylated peptide-HLA proteins and biotinylated DNA barcodes were mixed at a 3:1 molar ratio, and then complexed into fluorescently labelled multimers with PE-streptavidin or APC-streptavidin (Life Technologies, Carlsbad, CA) at 4:1 molar ratio of streptavidin to biotin. Each patient's peptide-HLA multimers were then pooled, concentrated, and used to stain cells.

Neoantigen-targeted TCRs were isolated from a patient's own peripheral blood. Briefly, PBMC were enriched for CD8 T cells by negative selection (Miltenyi Biotec, Bergisch Gladbach, Germany) with the addition of CD16 and CD56 markers (R&D systems, Minneapolis, MN) to prevent loss of activated CD8 T cells. Enriched CD8 T cells were then stained with the pooled library of neoantigen peptide-HLA multimers, plus a panel of fluorescently-labeled antibodies against cell surface markers, including CD39, CD103, and CD95 (see **Supplementary Table 4** for reagents, **Supplementary Figure 1** for gating strategy). Next, antigen-experienced CD95+, multimer+ CD8+ T cells expressing neoantigen-targeted TCRs were single-cell sorted using a FACSAria III (BD Biosciences, Franklin Lakes, NJ). DNA-barcodes from each sorted cell were sequenced and used to identify the TCR's neoantigen peptide-HLA binding target. TCR alpha and beta chains were amplified by RT-PCR and sequenced (MiniSeq or MiSeq, Illumina).

TCR alpha and TCR beta reads were used to identify V and J chains, and to reconstruct CDR3 sequences as well as full-length VDJ regions by leveraging IMGT library [69], with the MiXCR program [62].

Homology Directed Repair (HR) template generation

Paired TCRα/β variable regions from neoepitope-specific T cells were amplified by PCR using the corresponding variable region-specific primers. The purified PCR products were assembled with constant regions and homology arms to generate patient-specific HR template plasmids. The patient-specific HR template plasmid were designed to direct the integration of the gene cassette into the first exon of *TRAC*. The payload consisted of the following structure: P2A, HGH signal sequence, neoTCR β chain, furin cleavage site, P2A, Human Growth Hormone (HGH) signal sequence, neoTCR α variable region, and partial TRAC constant chain. Homology arm sequences homologous to the *TRAC* locus flanked the plasmid payload and were 1000 base pairs each. The templates were verified through Sanger sequencing and agarose gel electrophoresis.

NeoTCR T cell generation

CD4 and CD8 T cells were positively enriched from healthy donor leukapheresis products by magnetic selection (Miltenyi) and activated for 48 hours with CD3/CD28 stimulation (TransACT, 1:17.5 by volume; Miltenyi) in T cell medium (TexMACS medium, Miltenyi, supplemented with 12.5 ng/ml IL-7 and IL-15, Miltenyi, and 3% Human AB serum, Valley Biomedical, Winchester, VA). After activation, the T cells were centrifuged and resuspended in P3 buffer (Lonza, Basel, Switzerland). CRISPR/Cas ribonucleoproteins (RNPs) were formulated by complexing guide RNAs targeting *TRAC* and *TRBC* (Synthego, Redwood City, CA) to spCas9 protein (Aldevron, Fargo, ND) in a 6:1 molar ratio. The patient-specific HR template and RNPs were mixed with the

cell suspension, electroporated (Lonza, X-unit, EO-115), and transferred into T cell medium in a 24-well G-rex (Wilson Wolf, New Brighton, MN) for 4-5 days with media changes as needed.

NeoTCR binding and affinity analyses

Specific binding of the patient-specific neoTCR was confirmed by flow cytometry. Biotinylated peptide-HLA molecules were fluorescently labelled with PE-streptavidin (ThermoFisher) and Biotin-labelled Dextran (500 kDa, Nanocs) to generate a dextramer for staining as previously described [70]. Cells were stained with a fixable viability dye, the matched peptide-HLA dextramer to measure neoTCR binding, CD4, and CD8 (see **Supplementary Table 4** for reagents). Cells were permeabilized and stained intracellularly with 2A antibody to assess gene editing. Gene editing was confirmed if ≥ 5% of the T cells stained positive for 2A. TCR identity was confirmed if ≥ 5% of neoTCR+ T cells stained positive for the matched peptide-HLA dextramer. CD8-independent binding was confirmed when 2A+neoTCR+ binding on CD4+ T cells was ≥ to 50% of the 2A+neoTCR+ CD8+ T cells. Otherwise, edited CD4 T cells were considered to have weak or no binding (CD8-dependent). An affinity score was generated as a metric to further quantify CD8 dependent or independent binding with the following formula: Affinity score = (CD4+ NeoTCR+ 2A+/CD4+2A+) + (CD8+ NeoTCR+ 2A+/CD8+ 2A+). In general, this results in the following TCR calling: <0.25 = non-binders, 0.25-1.25 = CD8 dependent, and >1.25 = CD8 independent.

Plate-based antigen stimulation of neoTCR cells

Streptavidin-coated plates (Eagle Biosciences, Amherst, NH) were pre-incubated with cognate or control peptide-HLA molecules at various concentrations for 2-5 hours at room temperature or 16-30 hours overnight at 4˚C. T cells electroporated with neoTCRs or control TCRs were then stimulated on the plates in T cell culture medium (TexMACS + 3% Human AB serum + 1% Pen/strep, Gibco) at 37 ˚C and 5% CO_2.

IFNγ secretion and product selection

The supernatant from the plate-based stimulation assay (overnight using 0.1-1000 ng/ml peptide-HLA) was collected and analysed by CBA (Human Th1/Th2 Cytokine Kit II, BD Biosciences), acquired on an Attune NxT flow cytometer (Thermo Fisher), and an EC_{50} was calculated for IFNγ in GraphPad Prism. Product Selection was performed considering target truncality, expression, TCR functionality and neoantigen and HLA diversification.

Cell killing in a colorectal cancer cell line

A tumour biopsy and PBMCs were obtained from a treatment naïve patient with colorectal adenocarcinoma (Asterand Inc, Detroit MI, USA). A neoTCR was isolated from the PBMC sample using the targeting a mutation in COX6C (R20Q peptide aa18-46, HLA-A:02:01). The SW620 colorectal cancer cell line (CCL-227, ATCC) was transduced with IncuCyte NucLight Red Lentivirus (Sartorius) and sorted for high dye (red) expression. The SW620 cells were then transfected with gRNA and Cas9 ribonucleoproteins and single-stranded HDR template containing the desired neo-antigen point mutation (R20Q) and PAM-ablating mutation in cis under the control of the endogenous regulatory elements. Genotyping confirmed editing and clonal cell populations were isolated by limiting dilution cloning and single cell sorting. Wild-type or mutant SW620 cells, expressing endogenous levels of HLA and neoepitope, were then incubated with NeoTCR-specific T cells in an IncuCyte (Sartorius) for 24 hours to determine target cell killing.

Clinical manufacturing

Plasmid manufacturing. All clinical products were manufactured in the PACT Plasmid and Cell GMP manufacturing facilities (South San Francisco, CA) following clinical manufacturing protocols. NeoTCR-P1 plasmid was propagated from patient-specific HR template plasmid generated for TCR validation, using selected patient-specific HR template plasmid as

source material for GMP plasmid manufacturing. Patient-specific plasmid reagent was transformed into Escherichia Coli 5α (Aldevron) competent cells. Transfected cells were plated, and a single isolated colony was used for seed culture growth, then transferred to inoculate the main fermenter. The end of fermentation culture was collected and centrifuged to harvest cell paste. The cell paste was lysed, RNA enzymes digested, then clarified by flocculation and depth filtration. During purification, the clarified lysate was processed by anionic exchange chromatography (AEC) then hydrophobic interaction chromatography (HIC). Purified plasmid was concentrated and diafiltered into formulation buffer by hollow-fiber cartridge tangential flow filtration (TFF), sterile filtered, and frozen until cell manufacture.

Clinical cell manufacturing. Patient leukapheresis products were received from clinical sites after overnight shipment. CD4 and CD8 T cells were positively selected on the ClinicMACs Prodigy (Miltenyi). Up to 715 × 10^6 cells were seeded in culture media (TexMACS media + 3% Human AB Serum, V2.0; or PRIME-XV Media [Irvine Scientific, Santa Ana, CA], V2.1 or V3.0, see **Supplementary Table 3**), supplemented with cytokines (IL-7 and IL-15, each at 12.5 ng/ml) and activated for 44 hours with TransACT (1:17.5 by volume) in a G-Rex 100M CS (Wilson Wolf). Cells were then collected and electroporated on the Lonza Nuclefoector (LV-unit, EO-115, V2.0 or V2.1) or a pre-commercial version of the CTS Xenon Electroporation system (ThermoFisher, V3.0) with RNPs and patient-specific plasmid DNA to express a patient-specific neoTCR. Each individual lot was then expanded in a G-Rex in cytokine supplemented growth media (TexMACS media + 3% Human AB Serum, V2.0; or PRIME-XV Media + 2% Physiologix serum replacement [Nucleus Biologics, San Diego, CA], V2.1, V3.0), with media exchanges and splits to additional G-Rex vessels as appropriate. On day 13, cells were harvested and cryopreserved in a 50:50 mix of Plasma-Lyte-A (Baxter, Deerfield, IL) plus 2% human serum albumin (Grifols, Los Angeles, CA) and CS10 (Stemcell Technologies, Vancouver, Canada).

NeoTCR staining and T cell functional assays

IFNγ secretion at clinical lot release. An aliquot of fresh cells was taken on the day of harvest and tested using the plate-based stimulation assay described above (24 h stimulation). Controls consisted of "mismatch" peptide HLA coated plates. The supernatant was collected and analysed by IFNγ ELISA (Quantikine ELISA Human IFNγ Immunoassay Kit, R&D Systems) or using the ELLA Simple Plex Immunoassay platform (Simple Plex for Human IFNγ, Bio-techne, Minneapolis, MN). An EC_{50} was calculated in GraphPad Prism.

Proliferation assay. An aliquot of the cryopreserved final cell product was thawed, washed, and rested for three days in T cell recovery medium (TexMACS + 3% Human AB serum + 12.5 ng/ml IL-7 and IL-15). Rested cells were labelled with ViaFluor (Biotium, Fremont, CA) and incubated for 10 minutes at 37 ˚C, followed by a 30-minute incubation with stop solution (Day 0). ViaFluor stained cells were then used for the plate-based stimulation assay (0.1-1000 mg/ml peptide-HLA) for 22-26 hours, supplementing the media with 5 ng/ml IL-7 and IL-15. No stimulation, mis-matched peptide-HLA (1000 ng/ml) and TransACT (1:17.5) were used as controls. The next day (day 1), TransACT samples were washed 2X and all samples were removed from stimulation and transferred to a fresh plate in T cell culture medium and placed at 37 ˚C and 5% CO_2 for 72 hours (Day 4). Viafluor cells were taken on day 0 (pre-stimulation) or day 4 (post-stimulation) and stained for flow cytometric analysis (see **Supplementary Table 4** for reagents, **Supplementary Figure 2** for gating strategy). Cells were labelled with a fixable viability dye and stained with neoTCR-matched dextramer to measure neoTCR surface expression, CD8, CD4, and TCRαβ. Cells were then fixed, permeabilized, and stained intracellularly with the 2A antibody to assess total gene editing. Cells were fixed and acquired on the Attune NxT Flow Cytometer. Proliferation EC_{50} is defined as the neoantigen peptide-HLA concentration at which ViaFluor MFI reaches half of the minimum ViaFluor MFI when the dose-response curve is fitted with a sigmoidal trend.

Intracellular cytokine staining. An aliquot of thawed and rested cells from the proliferation assay were stimulated for 16 hours using the plate-based stimulation assay (0.1-1000 mg/ml peptide-HLA, 100,000 cells/well). No peptide-HLA was used as a control. T cell culture medium was supplemented with CD107a antibody, brefeldin A, and monensin protein secretion inhibitors. The next day, cells were stained with a fixable viability dye, and CD4 and CD8 surface markers, fixed and permeabilized, and stained intracellularly for IFNγ, TNFα, and IL-2 (see **Supplementary Table 4** for reagents, **Supplementary Figure 3** for gating strategy). Cells were fixed and acquired on the Attune NxT Flow Cytometer.

Flow cytometry analysis of neoTCR cells in manufactured products and peripheral blood

Cryopreserved T cell products or PBMC specimens were thawed, washed, and labelled with fixable viability dye. For identification of cells expressing the neoTCR, cells were incubated with a multimer reagent prepared using cognate peptide-HLA molecules [70], then stained with a panel of surface antibodies for pharmacokinetic analysis (see **Supplementary Figure 4** for gating strategy). Transgene expression was further identified by intracellular staining with the 2A peptide antibody. Additional staining for phenotypic markers was performed on thawed manufactured products or PBMC specimens (see **Supplementary Table 4** for a list of all flow reagents, and **Supplementary Figures 5-8** for gating strategies). Post-dose PBMC specimens were first enriched for neoTCR+ cells after peptide-HLA multimer staining using anti-APC magnetic enrichment beads (Miltenyi). neoTCR positive counts per µL were calculated using the following formula: absolute lymphocyte count x (% $CD5^+$ of live lymphocytes) x (% neoTCR positive of $CD5^+$). Matching absolute lymphocyte count data was not available for all timepoints. Data were acquired using an Attune NxT cytometer and analysis was performed using FlowJo (BD Biosciences) or FCS Express (De Novo Software, Pasadena, CA) software.

Serum Cytokine Analysis

Serum protein concentrations were measured by Precision for Medicine using an electrochemiluminescence immunoassay (Meso Scale Discovery, Rockville, MD). V-Plex Proinflammatory Panel 1 was used for the following cytokines: IFNγ, IL-2, IL-6, IL-8, IL-10, IL-12p70, IL-13, and TNFα. V-Plex Cytokine Panel 1 was used for the following cytokines: GM-CSF, IL-7, and IL-15. Single V-Plex and U-plex assays were used for IL-1RA and IL-2Rα, respectively. Analysis was performed using a MESO QuickPlex SQ 120 instrument and Discovery Workbench 4.0 software (Meso Scale Discovery).

Fluorescence microscopy of tumour FFPE sections

Tumour FFPE sections were imaged using RNAscope fluorescence *in situ* hybridization and immunofluorescence. RNAscope combined with immunofluorescence was performed using ACD's RNAscope Multiplex Fluorescent Detection Kit v2 (#323110, Advanced Cell Diagnostics, Newark, CA) combined with ACD's RNA-Protein Co-detection Ancillary Kit (#323180). The protocol was adapted from the vendor's documentation entitled, "RNAscope Multiplex Fluorescent v2 Assay combined with Immunofluorescence - Integrated Co-Detection Workflow (ICW)" (MK 51-150/Rev A/ Effective Date 10/05/2020). The ISH component of the assay uses the instructions in Chapter 4 of the RNAscope Multiplex Fluorescent Reagent Kit v2 User Manual (323100-USM). Vendor instructions were followed except for the following modifications: 1) Tris Buffer Saline with Tween 20 (1X) (Cell Signaling technology, Danvers, MA) was used instead of Phosphate Buffered Saline w/0.1% Tween-20 (1X); 2) 4% formaldehyde in PBS (formed from Pierce 16% formaldehyde) was used instead of 10% Neutral Buffered Formalin; 3) Fluoromount-G (SouthernBiotech, Birmingham, AL) was used instead of Prolong Gold Antifade mountant; and 4) CitriSolv was used instead of xylene. Sections were stained with anti-CD3 (clone EP4426, Abcam; anti-rabbit AF647, ThermoFisherVector2A RNAScope Probe to identify neoTCR edited cells (Advanced Cell Diagnostics; Opal 570, Akoya Biosciences, Marlborough, MA), and DAPI (ACD).

Statistical Analysis

No formal hypothesis was tested in the Phase 1 study. Design considerations were not made with regard to explicit power and type I error considerations, but were made to obtain preliminary safety, feasibility, PK, PD, and antitumor activity information in this population. Dose escalation was conducted in a traditional 3+3 design and each dose level was cleared with 3 patients treated with 3 TCRs. Measurements were taken from distinct samples. NeoTCR editing and IFNγ production at product release are reported as the average of two replicate tests from the same sample. For correlations, data was first tested for normal or log-normal distributions; Pearson correlations were performed on normally distributed data, otherwise, a Spearman correlation was performed. Additional statistical tests are indicated in each figure legend.

Data Availability

The following publicly available data sets were utilised: ExAc (3.1, http://exac.broadinstitute.org), dbSNP (v146, ftp://ftp.broadinstitute.org/bundle), GATK Resource Bundle (hg19/Grch37, ftp://ftp.broadinstitute.org/bundle), Human Proteome (Homo_sapiens.GRCh37.75.pep.all.fa, http://ensembl.org/), IMGT (TCR/HLA, 3.1.17, http://www.imgt.org/), RefSeq (1052019, ftp://hgdownload.cse.ucsc.edu/goldenPath), TCGA (Version 1.0, https://portal.gdc.cancer.gov/), Broad Institute (hg19, ftp://ftp.broadinstitute.org/bundle). The TCR sequences from the present study are available in the article supplemental files, and the genomics data is available on reasonable request from the European Genome-Phenome Archive (EGA) repository.

Acknowledgments

We thank the patients and their families and caregivers who participated in this study. We also thank present and previous PACT employees who contributed to this work including the Upstream Operations, Process Development, Plasmid Manufacturing, Cell Manufacturing, Clinical Development, Clinical Operations, Quality Control, Quality Assurance, and Program Management teams.

Funding

The work was funded by PACT Pharma. J.R.H. and A.R.R. are funded by the Parker Institute for Cancer Immunotherapy. A.R. is funded by National Institutes of Health grant R35 CA197633. D.Y.O. is supported by NIH K08AI139375, a Young Investigator Award from the Prostate Cancer Foundation, and the Damon Runyon Clinical Investigator Award (CI 110-21). K. M. C. is supported by the UCLA Tumor Immunology Training Grant (NIH T32CA009120), the Cancer Research Institute Irvington Postdoctoral Fellowship Program, and the V Family Foundation Gil Nickel Melanoma Research Fellowship.

Author Contributions

S.P.F., K.J., T.H., Z.P., E.S., C.L.W., W.L., A.V.R., S.J.M., and A.R.R. wrote the first draft of the manuscript. A.V.R, R.F., A.S., and T.S-S. designed, initiated, and ran the clinical study protocol. A.V.R, A.S, D.A.B., D.Y.O., B.C., M.A., Y.YY., A.J.S, J.A.S., and S.M.L enrolled, treated, and cared for patients on the clinical study protocol. Z.P., E.S., Y.M., K.M.C., C.S. performed and interpreted bioinformatics analysis. M.T.B., O.D. K.H., and M.C.Y. developed or conducted work related to peptide-HLA protein synthesis. C.L.W., S.P., M.T.B., D.A., and B.Y., B.B.Q created the

process, acquired, and/or analysed data for neoTCR T cell isolation. K.J., W.L., and R.M. developed the method or performed and analysed the studies for non-viral precision T cell receptor replacement. A.J.L. developed and conducted functional cytotoxicity experiments. B.S., A.C., and J.M. developed the methods, performed studies, and analysed or interpreted data for product selection. Cell and plasmid manufacturing processes were created and supervised by I.M., D.A., and L.D. Flow cytometry was performed, analysed, or supervised by S.P.F, T.H., S.G., E.Y.H., A.H., M.K., W.W., L.S., E.H., V.M., and B.P. (for the final cell product) and S.P.F., T.H., S.G., E.H., and A.H. (post-infusion). T.H. analysed serum cytokines. A.H.C.N. and Y.L. performed fluorescence microscopy and together with J.R.H. scored and interpreted the staining. S.P., M.T.B., A.F., S.J.M. D.B., J.R.H., and A.R.R. conceived the initial idea and provided scientific input for neoTCR cell isolation for personalized adoptive cell therapy. All authors proof-read and approved the final manuscript.

Competing interests

S.P.F., K.J., T.H., Z.P., E.S., Y.M., W.L., S.P., C.L.W., B.Y., O.D., K.H., B.S., A.C., M.T.B., I.M., W.W., M.K., S.G., E.H., A.H., D.A., A.J.L., B.B.Q., C.S., D.A., L.S., E.Y.H., V.M., J.M., L.D., B.P., R.M., M.C.Y., R.F., A.S., T.S-S., A.F., A.V.R, and S.J.M. were employees of PACT Pharma during the conduct of this work.

S.P., M.T.B., D.B., J.R.H. and A.R. are scientific co-founders of PACT Pharma.

K.M.C.. has received consulting fees from PACT Pharma and Tango Therapeutics and is a shareholder in Geneoscopy LLC.

D.Y.O. has received research support from Merck, PACT Pharma, the Parker Institute for Cancer Immunotherapy, Poseida Therapeutics, TCR2 Therapeutics, Roche/Genentech, and Nutcracker Therapeutics.

B.C. has advisory roles with: Iovance Biotherapeutics, IDEAYA Biosciences, Sanofi, OncoSec, Nektar, Genentech, Novartis and Instil Bio, and has received research funding from: Iovance Biotherapeutics, Bristol-Myers Squibb, Macrogenics, Daiichi Sankyo, Merck, Karyopharm Therapeutics, Infinity Pharmaceuticals, Advenchen Laboratories, Idera, Neon Therapeutics, Xencor, Compugen, PACT Pharma, RAPT Therapeutics, Immunocore, Lilly, IDEAYA Biosciences, Tolero Pharmaceuticals, Ascentage Pharma, Novartis, Atreca, Replimune, Instil Bio, Trisalus, and Kinnate.

J.A.S. reports honorarium with Iovance, Apixogen, Jazz Pharm, and research with BMS, PACT Pharma, and Corvus.

A.J.S. reports consulting/advising role to J&J, KSQ therapeutics, BMS, Enara Bio, Perceptive Advisors, and Heat Biologics, and Iovance Biotherapeutics. Research funding: GSK (Inst), PACT pharma (Inst), Iovance Biotherapeutics (Inst), Achilles therapeutics (Inst), Merck (Inst), BMS (Inst), Harpoon Therapeutics (Inst).

A.R. has received honoraria from consulting with Amgen, CStone, Merck, and Vedanta, is or has been a member of the scientific advisory board and holds stock in Advaxis, Appia, Apricity, Arcus, Compugen, CytomX, Highlight, ImaginAb, ImmPact, ImmuneSensor, Inspirna, Isoplexis, Kite-Gilead, Lutris, MapKure, Merus, PACT, Pluto, RAPT, Synthekine and Tango, has received research funding from Agilent and from Bristol-Myers Squibb through Stand Up to Cancer (SU2C), and patent royalties from Arsenal Bio.

D.A.B., A.H.C.N., Y.L., M.A., Y.Y. and S.M.L. report no conflicts of interest for this work.

Extended Data Figure Legends

Extended Data Figure 1. NeoTCR isolation, cytotoxicity, potency, gene editing and gene insertion. **a)** Neoantigen-specific T cell capture. **b)** NeoTCR specific killing of an SW620 COX6C-R20Q mutant colorectal cancer cell line. Healthy donor T cells engineered to express a neoTCR from the blood of a patient with colorectal cancer targeting the COX6C-R20Q mutation, cocultured with either the parental SW620 cell line (without R20Q mutation), or with SW620-COX6C R20Q. **c)** Potency (IFNγ EC_{50}) of neoTCRs isolated from the 16 patients compared with seven clinically active TCRs. **d)** Example gene editing (as measured by staining for 2A peptide) and neoTCR binding on CD4 and CD8 T cells for the three TCRs in a manufactured cell product. When transfected into CD8 T cells, all three TCRs expressed 2A and binding of dextramer, considered CD8-independent. TCR1033 and TCR1037 showed only 2A expression but no neoTCR binding by dextramer when transfected into CD4 T cells, considered CD8-dependent. **e)** Targeted locus amplification (TLA) was performed on 0010 TCR445 drug product. Primers specific for transgene and integrated transgene were used to amplify TLA processed genomic DNA. High coverage at the chromosome 14 integration site was observed (blue circle), indicating on-target *TRAC* transgene integration. A similar peak was not observed at chromosome 7, the site of TRBC knockout. **f)** Six clinical drug products from three patients were analysed using fluorescent *in-situ* hybridization (FISH) for chromosomal anomalies involving chromosome 7 and chromosome 14. All abnormal signals from each drug product tested were summed and compared to the total number of abnormal signals found in unedited cells from 10 separate donors. A p value was generated using an unpaired two-tailed t-test.

Extended Data Figure 2. Functionality of neoTCR engineered T cells. **a)** Intracellular cytokine staining upon activation with cognate peptide-HLA. NeoTCR T cells produce a polyfunctional cytokine profile on antigen encounter. Cells from the clinical final cell product were stimulated

overnight with plate-bound peptide-HLA. Percent of CD8 cells positive for the given markers is shown. **b and c)** T cells were stained with Viafluor membrane bound dye, stimulated with plate-bound peptide-HLA overnight, and proliferation measured 4 days later. **b)** Concentration-dependent proliferation of individual patient products. CD3/CD28 stimulation positive control indicated by [+] and mis-match compact negative control (used at 1000 ng/mL) indicated by [-]. Y-axis inverted; increased proliferation has lower ViaFluor MFI signal due to dilution of the dye after cell division. **c)** Leftward shift in the Viafluor MFI indicates increasing proliferation (left). Mis-matched peptide-HLA served as a negative control, and CD3/CD28 stimulation as a positive control (right).

Extended Data Figure 3. Characteristics of the manufactured product. **a)** Phenotype of CD4+ T cells (left) and CD8+ T cells (right) in incoming leukapheresis and final cell product from dosed patients. Bars represent individual NeoTCR-T cell products for each patient (up-to-3 neoTCRs per patient). For Dex+ CD4+ T cells, only products where the peptide-HLA multimer binds the inserted TCR in the absence of the CD8 co-receptor have data T cell subset abbreviations are as follows: EFF (effector), EM (effector memory), TM (transitional memory), CM (central memory), MSC (memory stem cell), N (naïve). **b)** T cell activation and phenotypic markers in the manufactured FCP. Percentage of CD4+ (top) or CD8+ (bottom) NeoTCR+ (left) or NeoTCR- (right) cells in the manufactured product that express the indicated surface markers. For NeoTCR+ CD4+ T cells, only products where the dextramer binds the inserted TCR in the absence of the CD8 co-receptor have data. **c)** NeoTCR knock-in efficiency of the endogenous TCR improved with changes in the manufacturing process. NeoTCR+ percentages were significantly different with the different process versions (***p=0.0006 by ANOVA; v2.1 and v3.0 were significantly better than process v2.0: *p = 0.0218 and **p=0.0029, respectively, by Tukey's multiple comparisons test, v2.0: n = 30, v2.1: n = 9, v3.0, n = 3). **d)** Cell counts of neoTCR+ cells

(left) and total cells (right) in manufacturing process v2.0 (n = 30) compared to process v2.1 (n = 9) and v3.0 (n = 3). Differences not significant (ns) by one-way ANOVA.

Extended Data Figure 4. Engineered neoTCR T cell delivery to patients. **a)** Absolute lymphocyte counts according to the original conditioning chemotherapy regimen (top), or the revised conditioning chemotherapy regimen (bottom). Patients treated with IL-2 combination therapy are indicated by dotted lines. **b)** Time to generate neoTCR T cell product for 16 dosed patients, ordered by consent date. * 0010: Due to COVID-19 shutdown in 2020 and updates to the manufacturing process, the patient underwent two apheresis and two manufactures of cell therapy products. # 0603: NeoTCR isolation was done three times for repeated attempts to find neoTCRs available for product selection. ^ 0026: Went through five separate PBMC samples before suitable neoTCRs were identified for product selection. ** 1003: Went through two manufactures of the cell therapy product. **c)** NeoTCR percentage (top) and counts (bottom) by dose level, separated by individual neoTCR (up to 3 per patient). Peripheral blood analysis of neoTCR cells in patients treated with dose level 1 (left), dose level 2 (centre), and dose level 3 (right). Total number of neoTCR cells was calculated per μL of blood per patient. Count information was not available for all timepoints. Patients treated with IL-2 are shown with dotted lines. **d)** Gene editing efficiency of final cell product correlates with neoTCR+ cells detected post-infusion. Percent of neoTCR+ cells infused in each patient (left; correlation Pearson r = 0.8463, ****P<0.0001). Percent of neoTCR+ cells infused per TCR (right; correlation Spearman r = 0.7475, ****P<0.0001). Area under the curve (AUC) was calculated from day 0 (pre-infusion) up to day 7. Data not shown for patient 0404; no day 0-7 post-infusion samples available.

Extended Data Figure 5. Post-infusion analysis of T cells in peripheral blood and serum cytokines. **a)** Serum cytokine levels measured using the MSD electrochemiluminescence platform. Thirteen cytokines were measured longitudinally. Horizontal dotted lines represent the

lower limit of quantification (LLOQ). IL-12 p70 (0411), IL-13 (0612), and GM-CSF (0038) were below the LLOQ for all but one patient (listed in parenthesis) and are not shown. IL-2 was detected only in patients treated with IL-2 combination therapy (0604, 0411, 0026). Samples measured but below LLOQ are entered as 0. No data for patients 0611, 0417 and 1003. **b)** Analysis of T cell phenotype of the final product and TCR transgenic cells recovered from blood of patients. Phenotype of dextramer+ CD8+ T cells in final cell product (left bars) compared to post-dose samples at 1-2 months after infusion (right bars). Final cell product phenotype shown here is the average of all the patients' products. **c)** T cell activation and phenotypic markers in the manufactured product compared to month 1-2 post-dose for a subset of patients. CD4 (left two columns) and CD8 (right two columns) are shown separately.

Extended Data Figure 6. Longitudinal retrospective analysis of epitope persistence, somatic signatures and ctDNA data. **a)** Venn diagrams of patients with longitudinal screening, pre and post infusion biopsies where available showing protein altering mutation overlap and targeted neoantigen persistence patterns. **b)** Somatic signature analysis of somatic exome mutations and their correlation with known somatic signatures in the COSMIC database. Signature 13 has previously been associated with APOBEC activity. **c)** Bespoke ctDNA assay for patient 506 at day -5 and day 0 timepoints showing truncal mutations in gray and targeted neoantigens in aqua and blue respectively. The PREP neoantigen (blue) is detectable by ctDNA and is at lower ctDNA concentrations than predicted truncal mutations.

Extended Data Figure 7. Tumour biopsy analyses and clinical responses. **a)** Retrospective analysis for HLA loss of heterozygosity (LOH, red fill) or no LOH (green fill). Each row is a neoTCR and columns are the HLA allele presenting its targeted epitope (A, B, C). TCGA study codes for the patients' tumor type are shown on the left. **b)** TCR and neoTCR CDR3 quantification in baseline and post-infusion biopsies. Absolute TCRα CDR3 reads from TCR assay were plotted.

BrCa: Breast Cancer, CRC: Colorectal Cancer, Mel: melanoma; DL1: Dose-level 1, DL3: Dose-level 3. Boxes indicate the interquartile range (IQR); centre line, median; whiskers, lowest and highest values within 1.5x IQR from the first and third quartiles, respectively. **c)** Schematic of the neoTCR CDR3 and its flanking barcode sequence that can be used to identify endogenous TCR or neoTCR specific reads. **d)** TCRs with a lower IFNγ EC_{50} at lot release (left, *p=0.0265) or higher TCR affinity score (right, *p=0.0152) were more frequently found in the post-infusion biopsy. Centre line is the median; p-value by un-paired two-tailed t-test. n=22; 16 found in the tumour, 6 not identified. For patient 0503, only the specific neoTCR sequence could not be determined. **e)** Correlation of percent of neoTCR cells from imaging versus corresponding sum of neoTCR CDR3 reads detected in post-infusion biopsies. Shaded grey representants the 95% confidence interval. The Pearson correlation coefficient was 0.8. **f)** Spider plot of the change in the sum of each patient's index lesions over time, relative to the baseline scan. No tumour assessment data for patient 0030 (skin lesions) or 0417. **g)** Computed tomography scans for patient 1003 at baseline (day -12, left panel) and on treatment (day 30, right panel).

1326
1327
1328

Methods References

50 Li, H. Aligning sequence reads, clone sequences and assembly contigs with BWA-MEM. *arXiv* https://doi.org/10.48550/arXiv.1303.3997 (2013).

51 Koboldt, D. C. *et al.* VarScan 2: somatic mutation and copy number alteration discovery in cancer by exome sequencing. *Genome research* **22**, 568-576, doi:10.1101/gr.129684.111 (2012).

52 Cibulskis, K. *et al.* Sensitive detection of somatic point mutations in impure and heterogeneous cancer samples. *Nat Biotechnol* **31**, 213-219, doi:10.1038/nbt.2514 (2013).

53 Saunders, C. T. *et al.* Strelka: accurate somatic small-variant calling from sequenced tumor-normal sample pairs. *Bioinformatics* **28**, 1811-1817, doi:10.1093/bioinformatics/bts271 (2012).

54 Lai, Z. *et al.* VarDict: a novel and versatile variant caller for next-generation sequencing in cancer research. *Nucleic Acids Res* **44**, e108, doi:10.1093/nar/gkw227 (2016).

55 Dobin, A. & Gingeras, T. R. Mapping RNA-seq Reads with STAR. *Curr Protoc Bioinformatics* **51**, 11 14 11-11 14 19, doi:10.1002/0471250953.bi1114s51 (2015).

56 Szolek, A. *et al.* OptiType: precision HLA typing from next-generation sequencing data. *Bioinformatics* **30**, 3310-3316, doi:10.1093/bioinformatics/btu548 (2014).

57 Reynisson, B., Alvarez, B., Paul, S., Peters, B. & Nielsen, M. NetMHCpan-4.1 and NetMHCIIpan-4.0: improved predictions of MHC antigen presentation by concurrent motif deconvolution and integration of MS MHC eluted ligand data. *Nucleic Acids Res* **48**, W449-W454, doi:10.1093/nar/gkaa379 (2020).

58 Favero, F. *et al.* Sequenza: allele-specific copy number and mutation profiles from tumor sequencing data. *Ann Oncol* **26**, 64-70, doi:10.1093/annonc/mdu479 (2015).

59 Roth, A. *et al.* PyClone: statistical inference of clonal population structure in cancer. *Nat Methods* **11**, 396-398, doi:10.1038/nmeth.2883 (2014).

60 Chang, M. T. *et al.* Accelerating Discovery of Functional Mutant Alleles in Cancer. *Cancer Discov* **8**, 174-183, doi:10.1158/2159-8290.CD-17-0321 (2018).

61 Power, R. P. *et al.* A diagnostic platform for precision cancer therapy enabling composite biomarkers by combining tumor and immune features from an enhanced exome and transcriptome. *Cancer Research* **80**, 1334 (2020).

62 Bolotin, D. A. *et al.* MiXCR: software for comprehensive adaptive immunity profiling. *Nat Methods* **12**, 380-381, doi:10.1038/nmeth.3364 (2015).

63 Diaz-Gay, M. *et al.* Mutational Signatures in Cancer (MuSiCa): a web application to implement mutational signatures analysis in cancer samples. *BMC Bioinformatics* **19**, 224, doi:10.1186/s12859-018-2234-y (2018).

64 Alexandrov, L. B. *et al.* The repertoire of mutational signatures in human cancer. *Nature* **578**, 94-101, doi:10.1038/s41586-020-1943-3 (2020).

65 Smith, C., Ma, Y., Campbell, K. M., Pan, Z. & Stawiski, E. Uncovering HLA loss of heterozygosity in cancer for the improvement of personalized neoTCR immunotherapy with PACT-ESCAPE. *Proc American Association for Cancer Research*, Abstract 1213 (2022).

66 Robinson, J. *et al.* IPD-IMGT/HLA Database. *Nucleic Acids Res* **48**, D948-D955, doi:10.1093/nar/gkz950 (2020).

67 Bratman, S. V. *et al.* Personalized circulating tumor DNA analysis as a predictive biomarker in solid tumor patients treated with pembrolizumab. *Nat Cancer* **1**, 873-881, doi:10.1038/s43018-020-0096-5 (2020).

68 Lybarger, L. *et al.* Enhanced immune presentation of a single-chain major histocompatibility complex class I molecule engineered to optimize linkage of a C-

terminally extended peptide. *J Biol Chem* **278**, 27105-27111, doi:10.1074/jbc.M303716200 (2003).

69 Lefranc, M. P. *et al.* IMGT(R), the international ImMunoGeneTics information system(R) 25 years on. *Nucleic Acids Res* **43**, D413-422, doi:10.1093/nar/gku1056 (2015).

70 Bethune, M. T., Comin-Anduix, B., Hwang Fu, Y. H., Ribas, A. & Baltimore, D. Preparation of peptide-MHC and T-cell receptor dextramers by biotinylated dextran doping. *BioTechniques* **62**, 123-130, doi:10.2144/000114525 (2017).

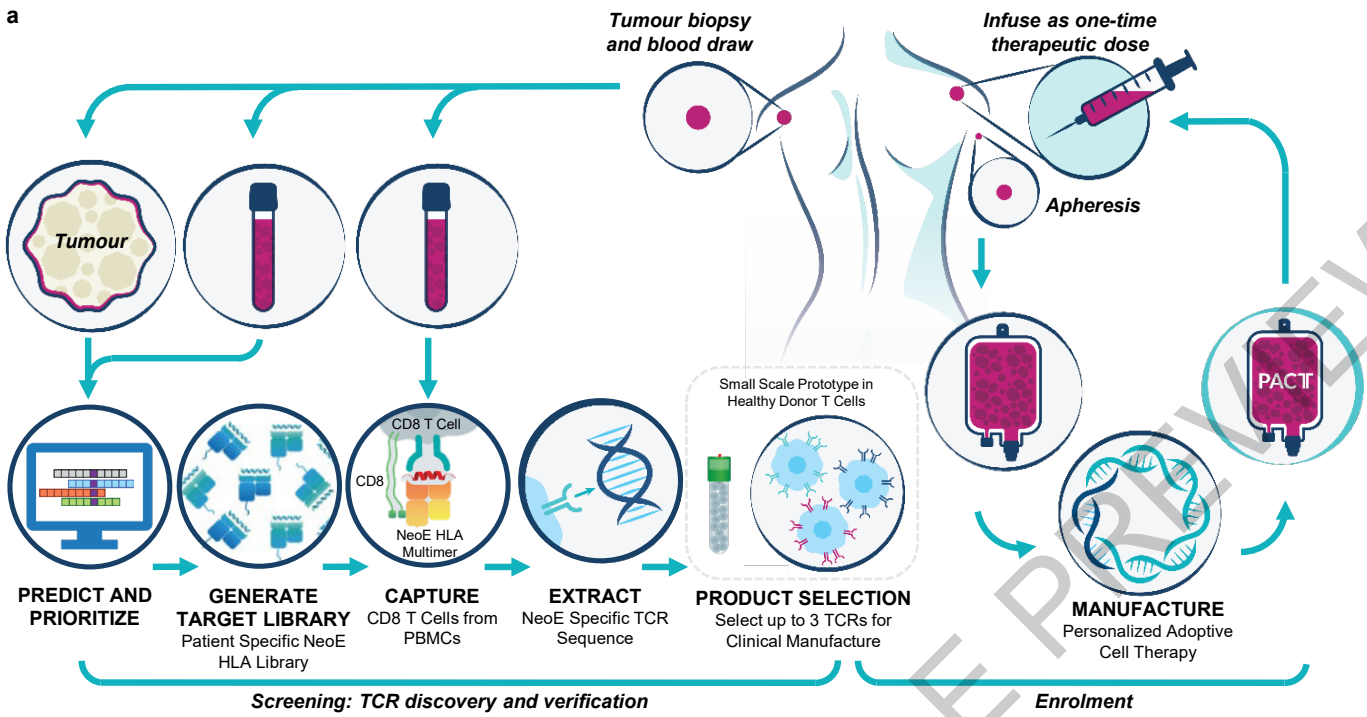

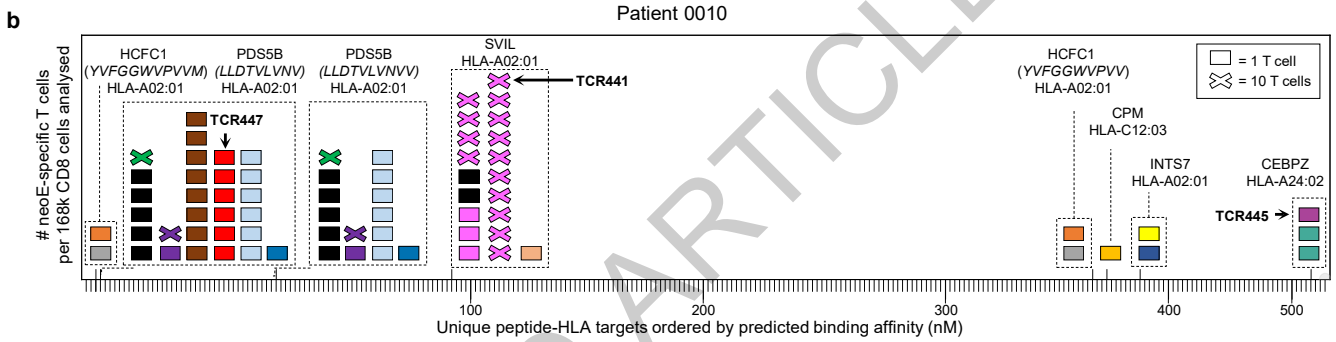

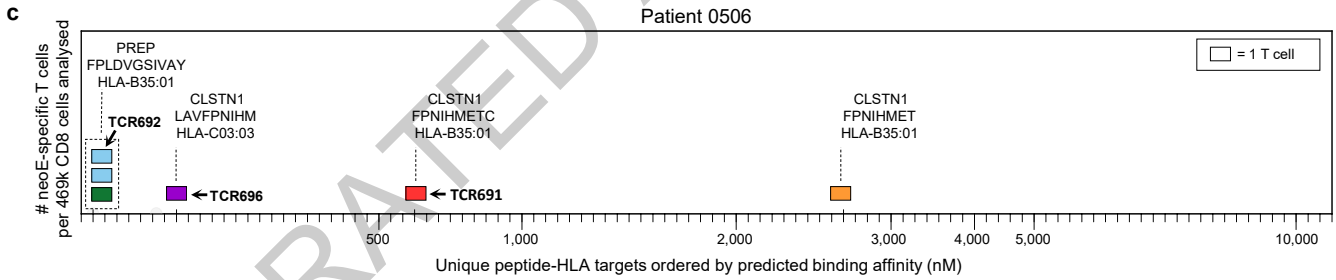

Figure 1

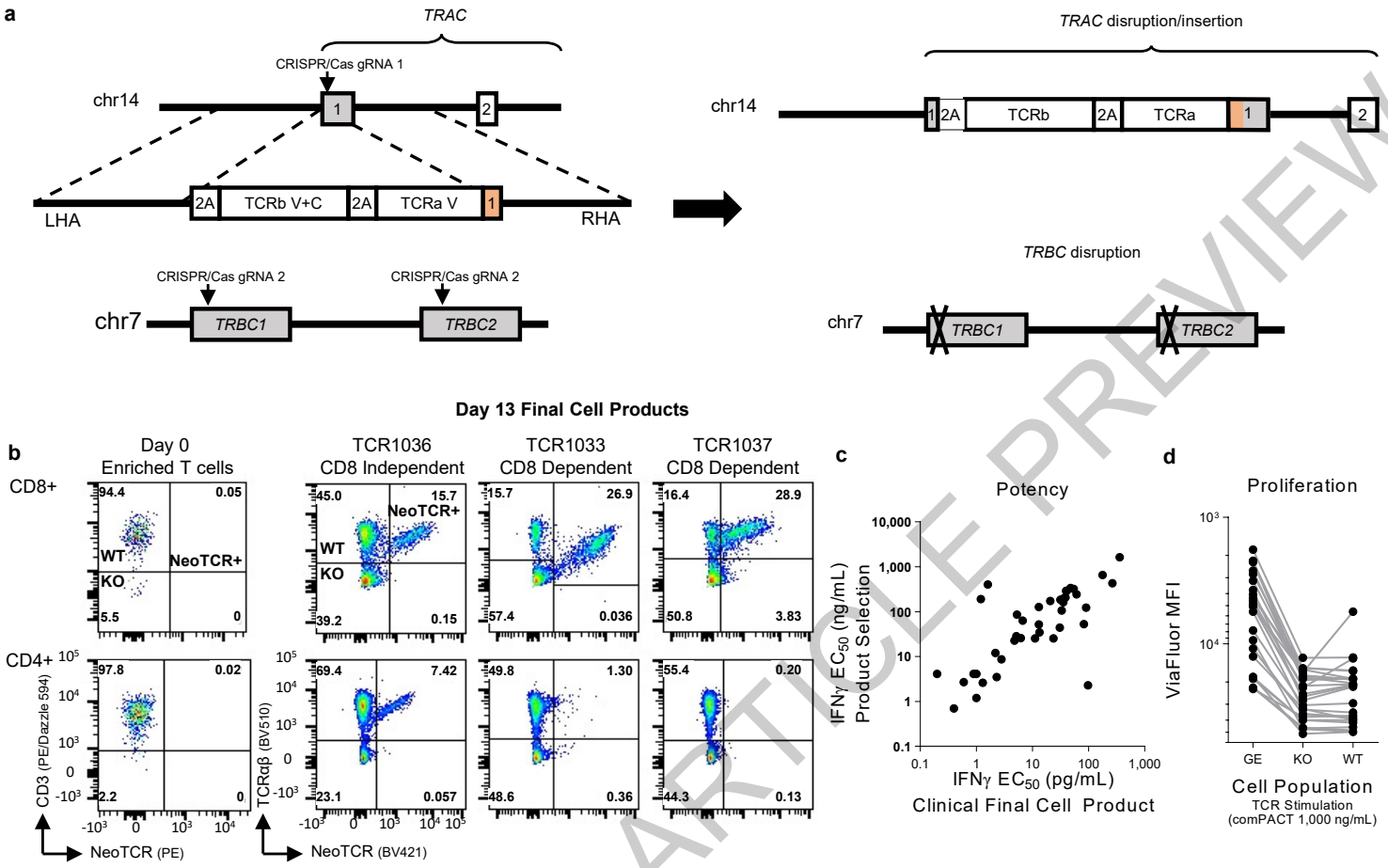

Figure 2

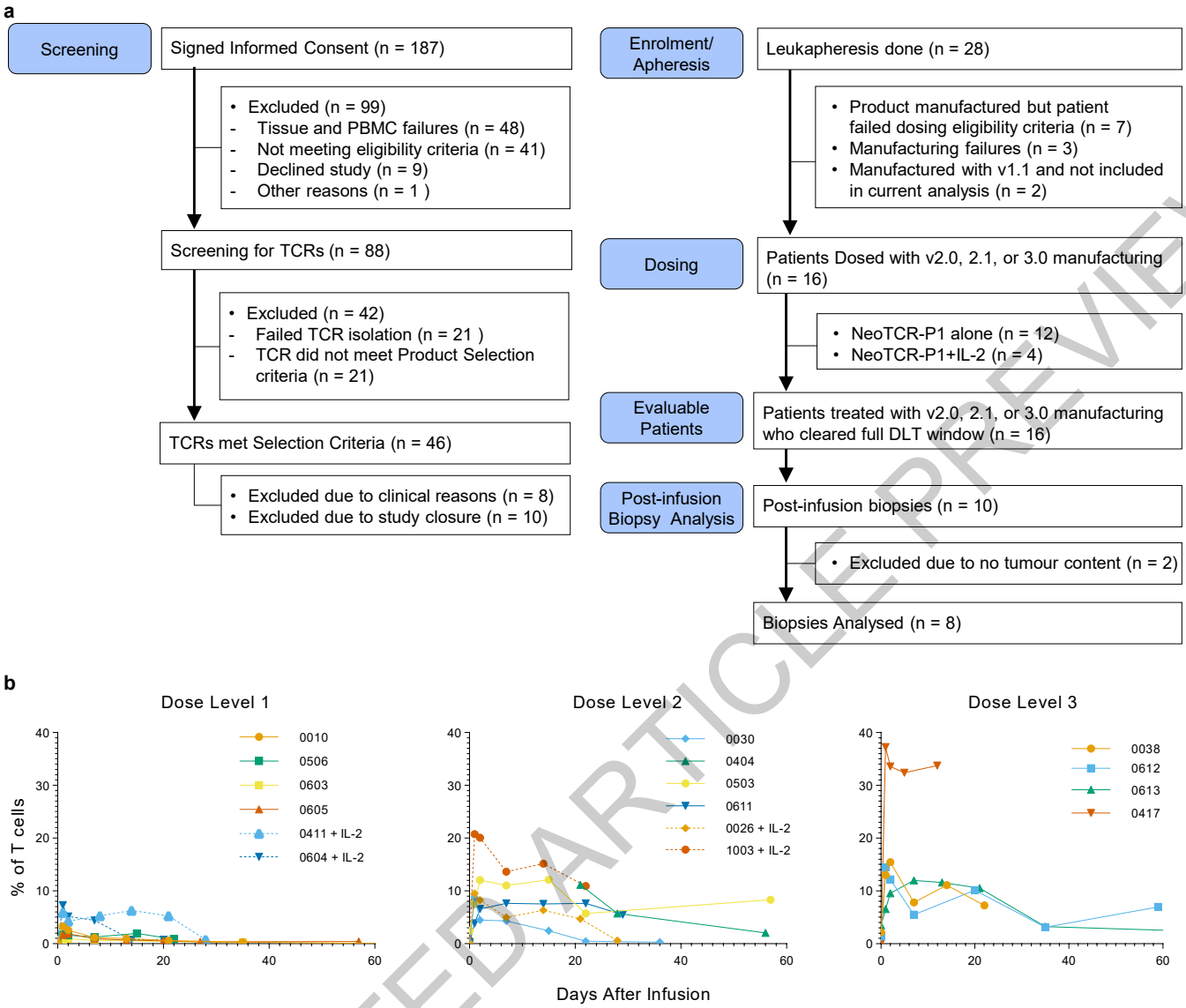

Figure 3

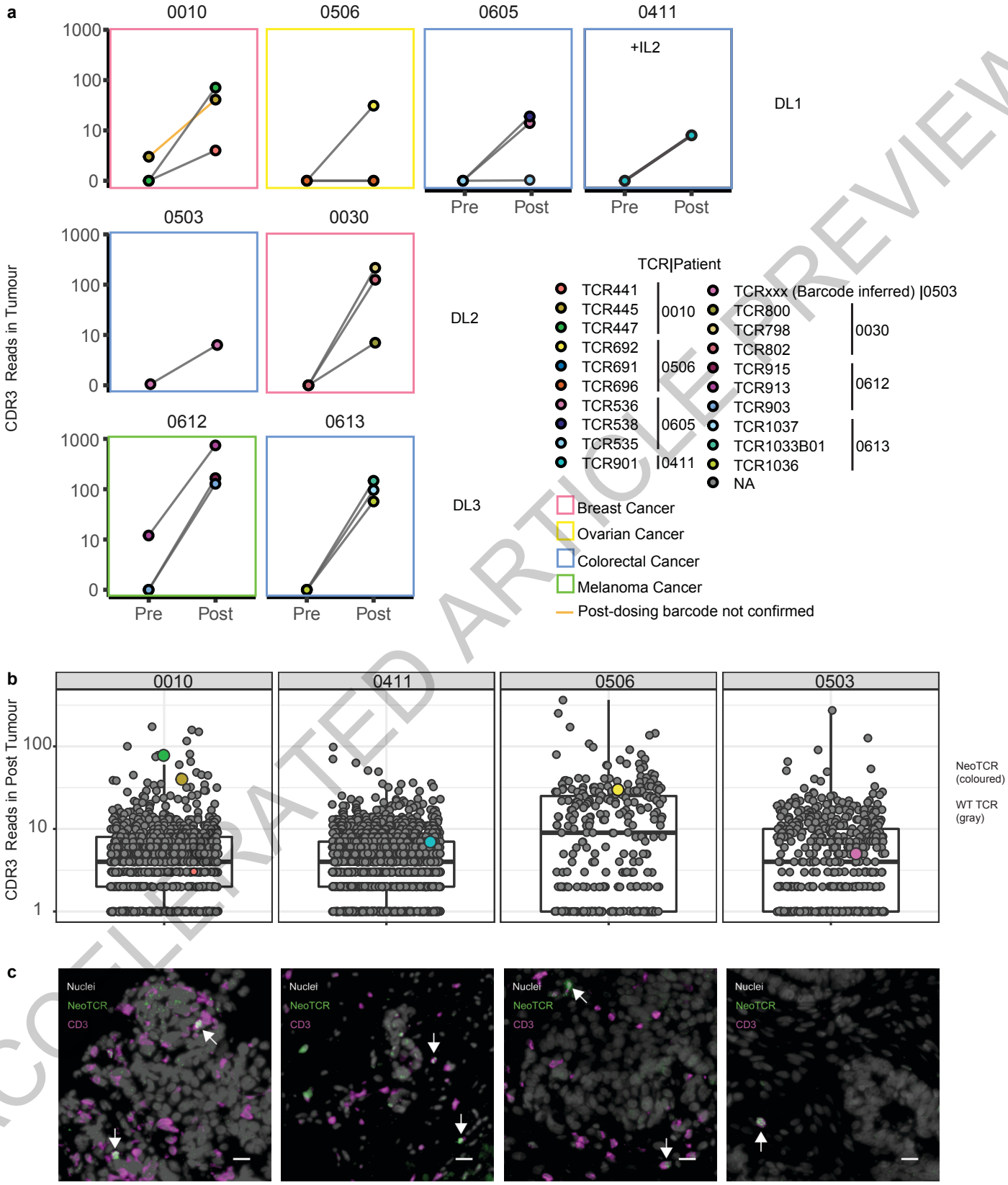

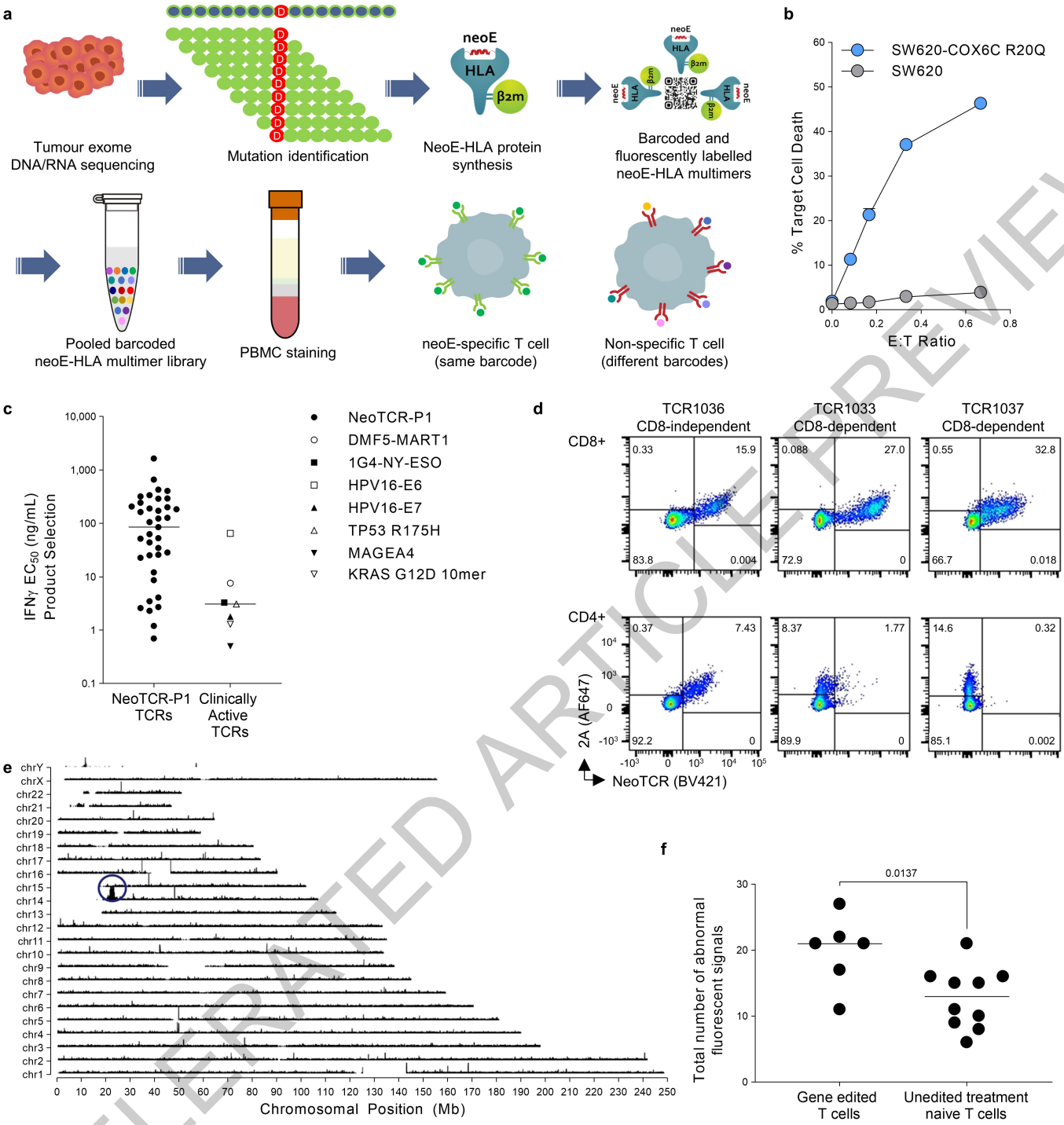

Extended Data Fig. 1

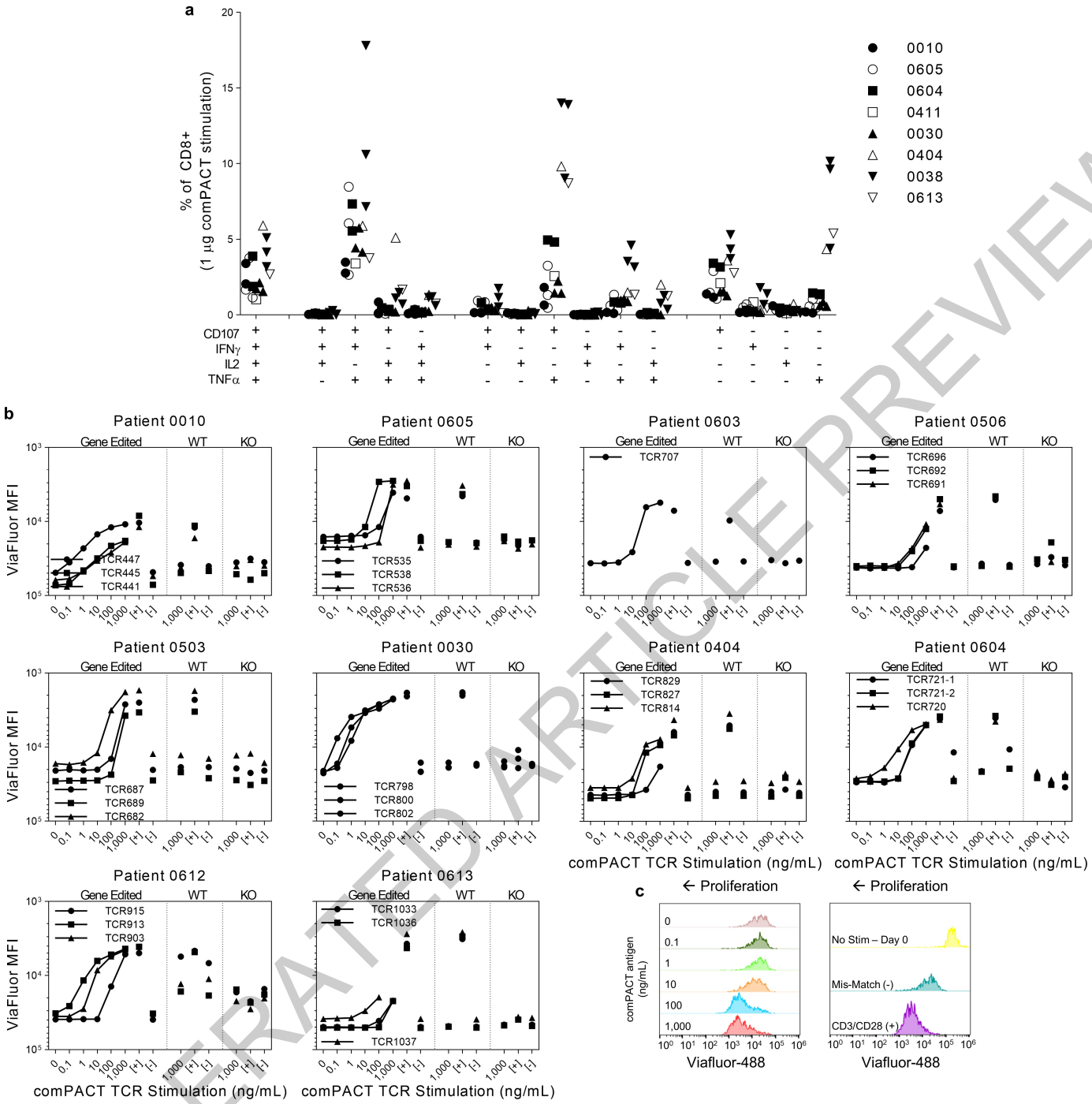

Extended Data Fig. 2

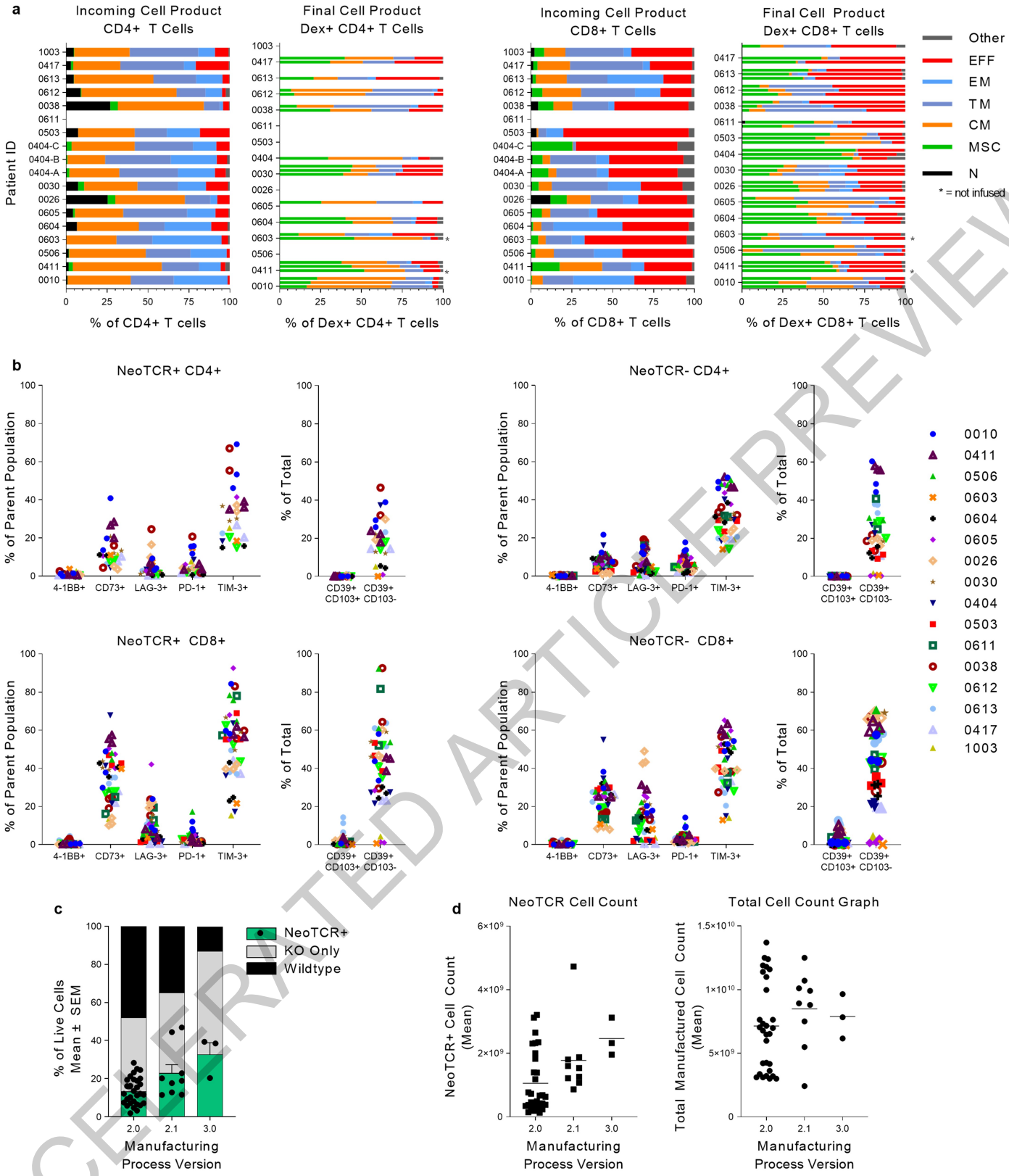

Extended Data Fig. 3

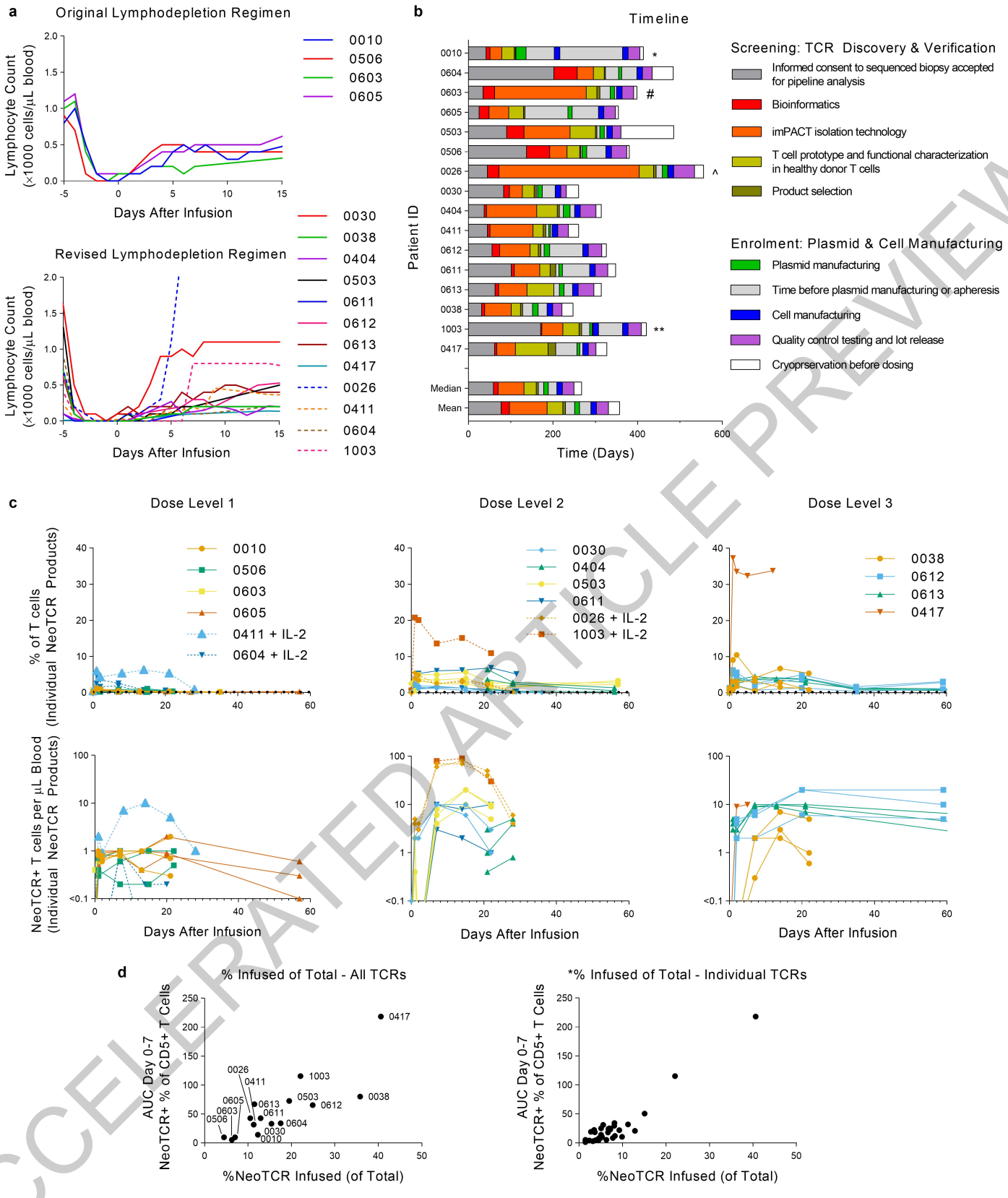

Extended Data Fig. 4

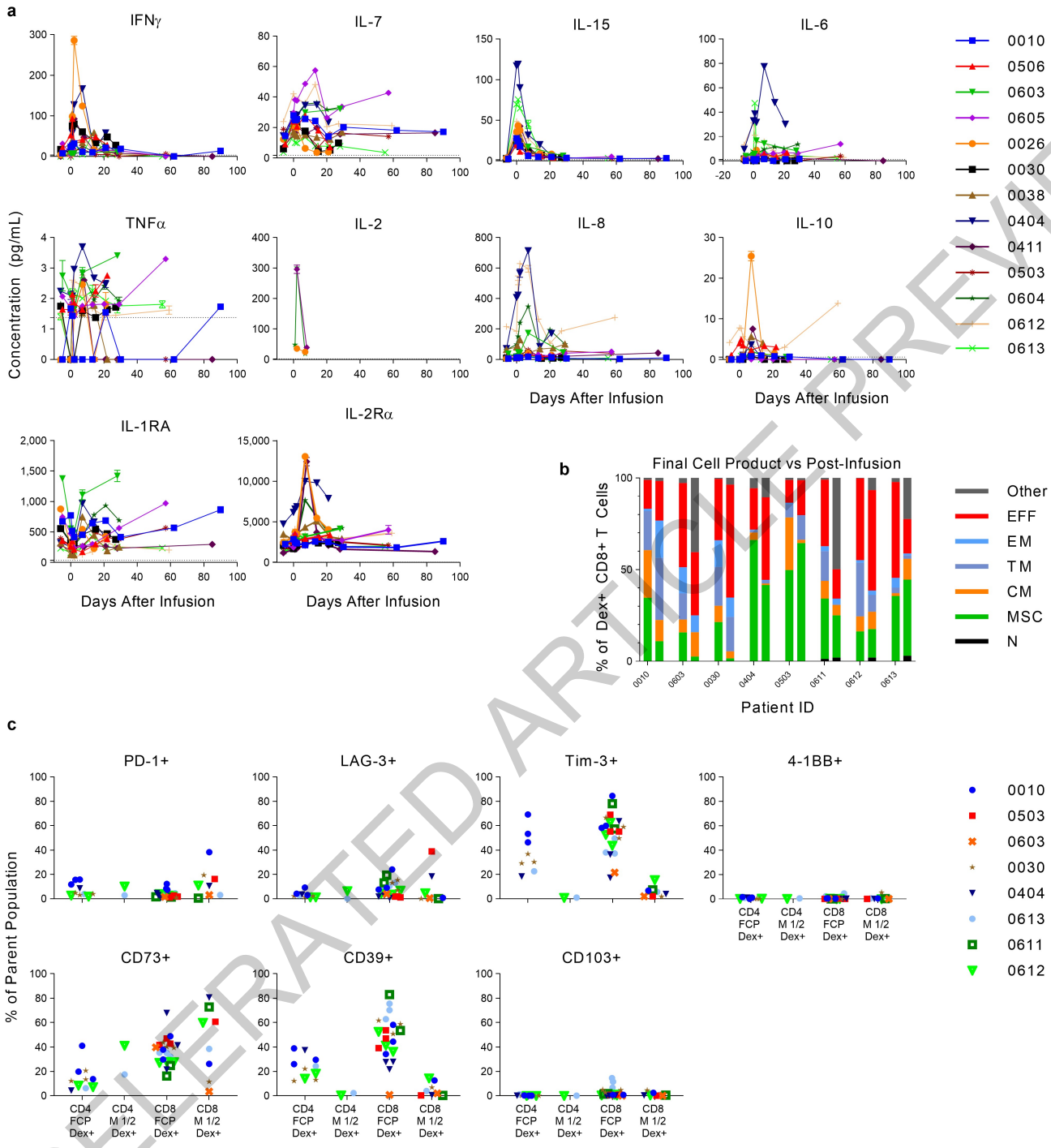

Extended Data Fig. 5

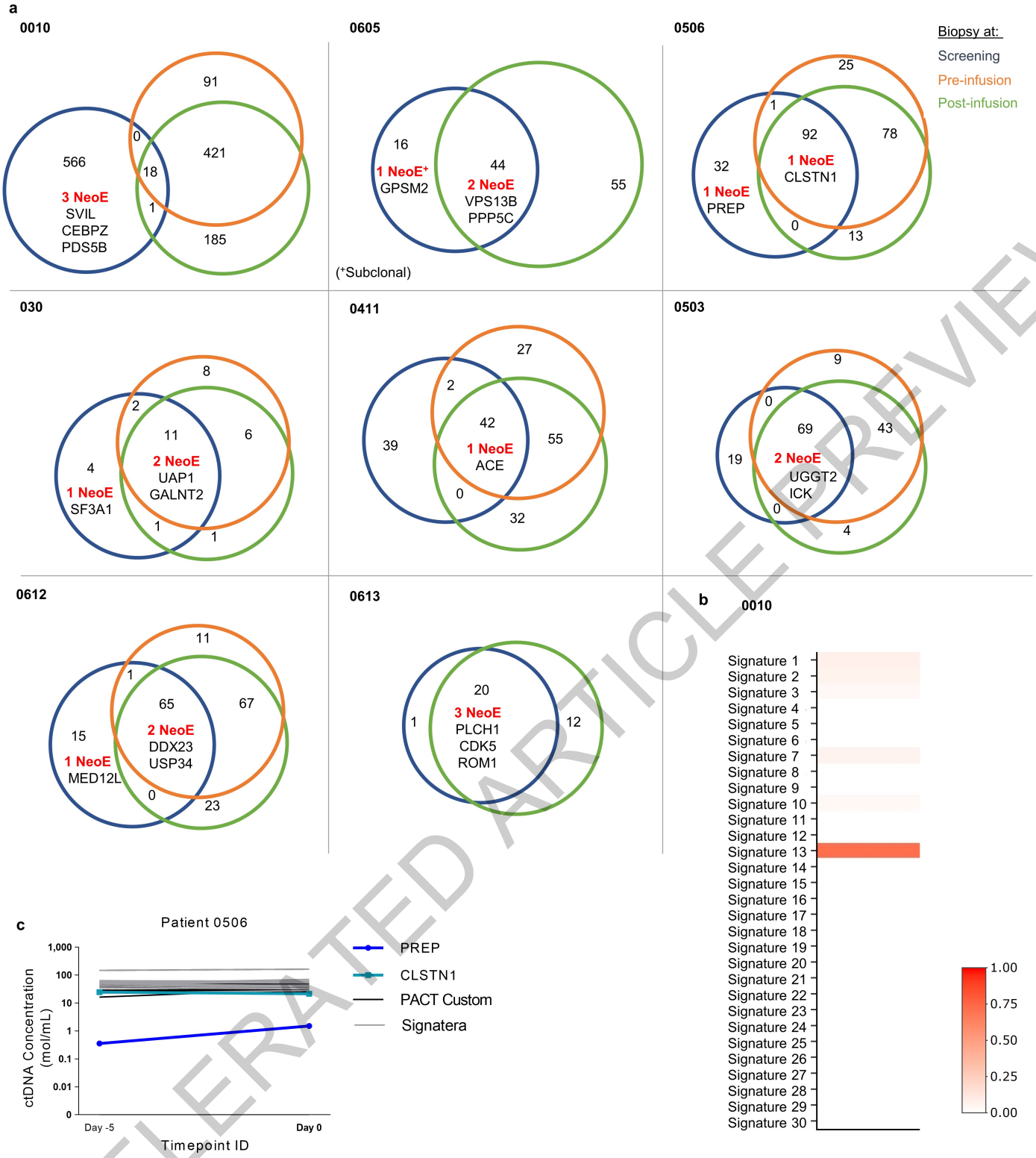

Extended Data Fig. 6

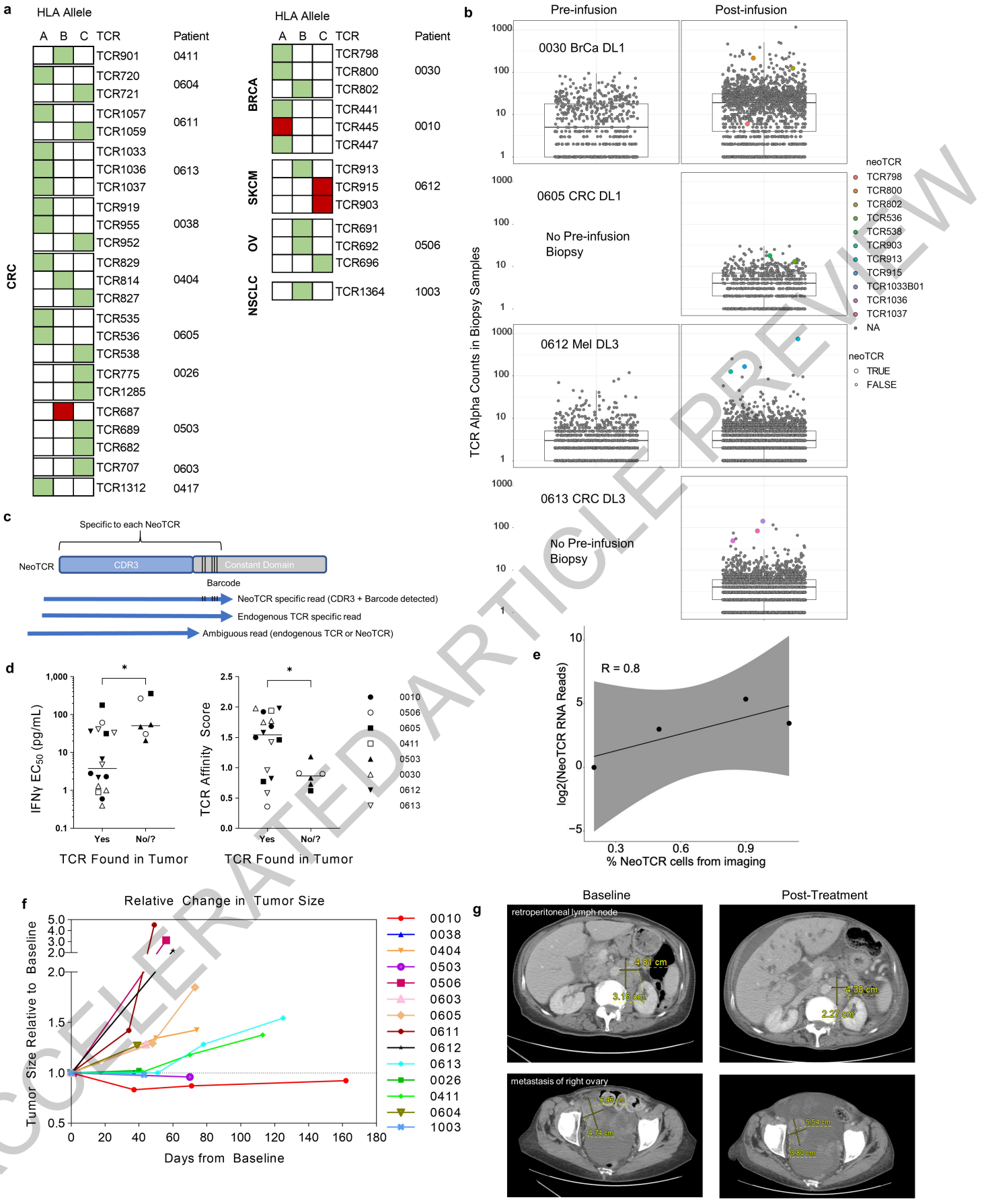

Extended Data Fig. 7

Extended Data Table 1 | Mutational load, predicted neoantigen peptide-HLA capture reagents, recognized mutations and TCR clonotypes for the 16 patients infused in the clinical trial. NSM = non-synonymous somatic mutations. TMB = tumour mutational burden and was calculated as follows: TMB=#NSM/35 MB, where 35 MB is the length of the sequencing footprint.

Dose level	Patient ID	# NSM (TMB)	# expressed mutations	HLA alleles covered by HLA library	# HLA-neoantigen capture reagents proposed*	# HLA-neoantigen capture reagents produced	# recognized neoantigens †	# unique TCRs isolated‡	# unique TCRs confirmed §
DL 1	0010	468 (13.4)	236	A*02:01, A*24:02, B*35:02, C*12:03	352	262	6	15 (11)	6
	0605	60 (1.7)	23	A*02:01, A*24:02, C*01:01, C*03:03	86	49	4	6	3
	0603	202 (5.8)	88	A*26:01, B*42:01, B*44:02, C*05:01, C*17:01	288	66	3	9 (3)	2
	0506	125 (3.6)	56	A*24:02, B*35:01, B*46:01, C*01:02, C*03:03	352	105	4	5	5
DL 2	0503	88 (2.5)	30	A*24:02, B*39:01, B*52:01, C*07:02, C*12:02	352	130	5	9 (8)	4
	0030	29, 31 (0.9)	20	A*02:01, A*11:01, B*35:01, C*04:01	352	117	7	10 (8)	7
	0404	120 (3.4)	35	A*01:01, A*31:01, B*08:01, B*40:01, C*03:04, C*07:01	352	94	3	7 (6)	6
	0611	74 (2.1)	25	A*01:01, A*24:02, B*57:01, C*04:01, C*06:02	352	67	4	8	4
DL 3	0038	95 (2.7)	34	A*02:01, A*24:02, B*07:02, B*51:01, C*15:02, C*07:02	352	125	10	30 (16)	9
	0612	244 (7.0)	81	A*01:01, B*08:01, B*07:02, C*07:01, C*07:02	352	126	3	16 (14)	3
	0613	43 (1.2)	21	A*02:01, C*07:02	352	83	5	8	6
	0417	107 (3.1)	62	A*02:01, A*25:01, B*15:01, B*18:01, C*03:03, C*12:03	352	147	11	17 (10)	6
NeoTCR-P1 + IL-2	0604	102 (2.9)	30	A*01:01, A*11:01, B*08:01, B*35:01, C*04:01, C*07:01	352	98	3	3	2
	0411	83 (2.4)	32	A*01:01, A*02:01, B*07:02, B*57:01, C*06:02, C*07:02	352	87	5	5	3
	0026	89 (2.5)	48	A*01:01, B*08:01, C*07:01	352	35,104	6	22 (11)	4
	1003	172 (4.9)	94	A*02:01, A*26:01, B*15:01, B*35:01, C*03:04, C*04:01	352	146	5	5	3
Median		102 (2.9)	35	5	352	104	5	8	4
Total				34 (unique)	5302	1841	84	175 (127)	73

*A maximum of 352 predicted neoantigen capture reagents were provided for protein synthesis.
†Number of unique non-synonymous somatic mutations recognized by one or more TCRs isolated from patient PBMCs.
‡Number of unique TCRs isolated from the patient PBMCs, number in parenthesis indicates the numbers that were passed on for confirmation, if it was less than the total number of unique TCRs isolated.
§Number of unique TCRs that were transfected into healthy donor cells and showed specific binding to the matched peptide-HLA and IFNγ secretion with peptide-HLA stimulation.
drome; SD: Stable Disease; PD: Progressive Disease; Y/N: Yes/No.

Extended Data Table 2 | Targeted neoantigen, manufacturing process, neoTCR transfection efficiency and function for each clinical infused product to the 16 patients in this cohort.

Dose level	Patient ID	Cell manufacturing process version	Gene	mRNA transcript per million (TPM) at screen	HLA Allele	Selected TCR ID	IFNγ EC_{50} (at lot release, pg/mL)*	NeoTCR+ T cells (as % of live)*
DL1	0010	2.0	SVIL	2.8	A*02:01	TCR441	5	11.6
			CEBPZ	2.3	A*24:02	TCR445	1	12.1
			PDS5B	0.6	A*02:01	TCR447	101	16.2
	0605	2.0	VPS13B	5	A*02:01	TCR535	362	9.3
			PPP5C	52	A*24:02	TCR536	177.9	7.4
			GPSM2†	271	C*03:03	TCR538	31.6	6.0
	0603	2.0	TENM4	1	C*05:01	TCR707	39.8	6.5
	0506	2.0	PREP	24	B*35:01	TCR692	61.5	1.9
			CLSTN1	45	B*35:01	TCR691	30.9	10.2
			CLSTN1	45	C*03:03	TCR696	266.4	17
DL2	0503	2.0	UGGT2	61	C*12:02	TCR682	20.8	19.6
			ICK	36	C*12:02	TCR689	48.1	19.3
			ICK	36	B*39:01	TCR687	54.6	21.3
	0030	2.0	UAP1	25	A*02:01	TCR798	1	12
			GALNT2	29	B*35:01	TCR802	1.3	16.1
			SF3A1	5	A*02:01	TCR800	0.4	15.4
	0404	2.0	STRADA	9	A*01:01	TCR829	38.9	25.2
			MTHFR	51	B*40:01	TCR814	6.2	20.1
			STRADA	9	C*07:01	TCR827	13	28.3
	0611	2.0	CDAC1	10	A*24:02	TCR1057	82.6	4.7
			FCGRT†	1	C*06:02	TCR1059	35.7	18.9
DL3	0038	2.1	NAALADL2	47	A*02:01	TCR919	1.6	46.8
			BRPF1	8	A*24:02	TCR955	5.3	44.4
			PAPSS1	39	C*07:02	TCR952	1.2	20.2
	0612	2.1	DDX23	38	B*08:01	TCR913	2.2	17.6
			USP34	67	C*07:02	TCR903	6.7	22.9
			MED12L	14	C*07:02	TCR915	36.3	18.9
	0613	2.1	PLCH1	25	A*02:01	TCR1036	41.2	11.4
			CDK5	18	A*02:01	TCR1033	33.2	12.8
			ROM1	5	A*02:01	TCR1037	4.8	11.6
	0417	3.0	RASA3	125	A*02:01	TCR1312	19.2, 25.8	40.0, 38.0
NeoTCR-P1 + IL-2	0604	2.0	WDFY3	14	A*11:01	TCR720	5.2	11.2
			MAN2A2	132	C*04:01	TCR721	90.9	23.2, 24.6‡
	0411	2.0	ACE	44	B*57:01	TCR901	0.9	13.5, 8.0, 3.2‡
	0026	2.0	ETNK1	159	C*07:01	TCR1285	23.7, 11.2	5.7, 7.1
			PRCC	85	C*07:01	TCR775	13.4	7.1
	1003	3.0	KBTBD3	18	B*35:01	TCR1364	98.7§	20.3

* Multiple values listed when more than one cell product lot was manufactured with the same TCR.
† Predicted subclonal mutation.
‡ Lot not infused; intended dose level reached without infusion.
§ IFNγ measured using the ELLA Simple Plex; all other reported values measured by IFNγ ELISA

Extended Data Table 3 | Patient and disease characteristics, adverse events and response assessment.

Dose level	Patient ID	Age	Cancer	# Prior regimens	# TCRs	Conditioning regimen	Total NeoTCR+ cell dose	Any AEs ≥ grade 3 and SAEs	TCR-related AEs	Response
DL 1	0010	38	HR+ Breast	7	3	Cy 300 mg/m^2 x3d Flu 30 mg/m^2 x3d	4 × 10^8	G3 neutropenia		SD (target lesions ↓ 17%) for 4m
	0605	53	MSS-CRC	4	3	Cy 300 mg/m^2 x3d Flu 30 mg/m^2 x3d	4 × 10^8	SAE D52 small bowel obstruction		PD
	0603	65	MSS-CRC	4	1	Cy 300 mg/m^2 x3d Flu 30 mg/m^2 x3d	2 × 10^8	COVID-19 + pneumonia		PD
	0506	70	Ovarian	6	3	Cy 300 mg/m^2 x3d Flu 30 mg/m^2 x3d	4 × 10^8	G3 neutropenia		PD
DL 2	0503	48	MSS-CRC	9	3	Cy 600 mg/m^2 x3d Flu 30 mg/m^2 x4d	1.3 × 10^9	G4 neutropenia SAE: UTI D74		PD
	0030	45	HR+ Breast	5	3	Cy 600 mg/m^2 x3d Flu 30 mg/m^2 x4d	1.3 × 10^9	G4 neutropenia		SD at D28 and D56
	0404	47	MSS-CRC	7	3	Cy 600 mg/m^2 x3d Flu 30 mg/m^2 x4d	1.3 × 10^9	G4 neutropenia SAE G3 Peri-hepatic hematoma		PD
	0611	44	MSS-CRC	5	2	Cy 600 mg/m^2 x3d Flu 30 mg/m^2 x4d	9 × 10^8	G2 Headaches week 2		PD
DL 3	0038	39	MSS-CRC	2	3	Cy 600 mg/m^2 x3d Flu 30 mg/m^2 x4d	4 × 10^9	G4 neutropenia		PD
	0612	47	Melanoma	3	3	Cy 600 mg/m^2 x3d Flu 30 mg/m^2 x4d	4 × 10^9	G4 neutropenia		PD
	0613	36	MSS-CRC	3	3	Cy 600 mg/m^2 x3d Flu 30 mg/m^2 x4d	4 × 10^9	SAE: G4 febrile neutropenia	G1 CRS	SD at D28 and D56
	0417	38	MSS-CRC	4	1	Cy 600 mg/m^2 x3d Flu 30 mg/m^2 x4d	5.4 × 10^9	SAE: G4 Hyponatremia SAE: G5 Malignant neoplasm progression		No post-baseline assessment
NeoTCR-P1 + IL-2	0604	40	MSS-CRC	5	2	Cy 600 mg/m^2 x3d Flu 30 mg/m^2 x4d	4 × 10^8 + IL-2	G3 neutropenia and febrile neutropenia; SAE: G3 pancreatitis D40		PD
	0411	58	MSS-CRC	5	1	Cy 600 mg/m^2 x3d Flu 30 mg/m^2 x4d	7.5 × 10^8 + IL-2	G4 neutropenia		SD at D28 and D56
	0026	58	MSS-CRC	5	2	Cy 600 mg/m^2 x3d Flu 30 mg/m^2 x4d	1.3 × 10^9 + IL-2	G4 neutropenia		PD
	1003	68	NSCLC	3	1	Cy 600 mg/m^2 x3d Flu 30 mg/m^2 x4d	1.96 × 10^9 + IL-2	G3 encephalopathy	G3 encephalopathy	SD at D28

MSS-CRC: Microsatellite Stable Colorectal Cancer; HR: Hormone Receptor; G: Grade; SAE: Serious Adverse Event; CRS: Cytokine Release Syndrome; SD: Stable Disease; PD: Progressive Disease; Y/N: Yes/No.

nature portfolio

Corresponding author(s): Antoni Ribas

Last updated by author(s): Oct 29, 2022

Reporting Summary

Nature Portfolio wishes to improve the reproducibility of the work that we publish. This form provides structure for consistency and transparency in reporting. For further information on Nature Portfolio policies, see our Editorial Policies and the Editorial Policy Checklist.

Statistics

For all statistical analyses, confirm that the following items are present in the figure legend, table legend, main text, or Methods section.

n/a	Confirmed
☐	☒ The exact sample size (*n*) for each experimental group/condition, given as a discrete number and unit of measurement
☐	☒ A statement on whether measurements were taken from distinct samples or whether the same sample was measured repeatedly
☐	☒ The statistical test(s) used AND whether they are one- or two-sided *Only common tests should be described solely by name; describe more complex techniques in the Methods section.*
☒	☐ A description of all covariates tested
☐	☒ A description of any assumptions or corrections, such as tests of normality and adjustment for multiple comparisons
☐	☒ A full description of the statistical parameters including central tendency (e.g. means) or other basic estimates (e.g. regression coefficient) AND variation (e.g. standard deviation) or associated estimates of uncertainty (e.g. confidence intervals)
☐	☒ For null hypothesis testing, the test statistic (e.g. *F*, *t*, *r*) with confidence intervals, effect sizes, degrees of freedom and *P* value noted *Give P values as exact values whenever suitable.*
☒	☐ For Bayesian analysis, information on the choice of priors and Markov chain Monte Carlo settings
☒	☐ For hierarchical and complex designs, identification of the appropriate level for tests and full reporting of outcomes
☐	☒ Estimates of effect sizes (e.g. Cohen's *d*, Pearson's *r*), indicating how they were calculated

Our web collection on statistics for biologists contains articles on many of the points above.

Software and code

Policy information about availability of computer code

Data collection	Flow cytometry data was collected using BD FACSDiva (V8.0.3) and analysed with FlowJo (V10.7.1 or V10.8.1), or FCS Express (V6.6.21.0). Serum cytokine analysis was performed using a MESO QuickPlex SQ 120 instrument and Discovery Workbench 4.0 software.
Data analysis	The following software was used for analysis (Version and or location listed in parenthesis): OptiType (1.3.4), netMHCpan (3.0, 4.0, or 4.1 as indicated in the methods), RSEM (1.3.3), STAR (2.7.6a), MiXCR (2.1.3), VarDictJava (1.8.2), VarScan (2.4.4), Sentieon (BWA, 201911.01), Sequenza (3.0), Strelka2 (2.9.10), Mutect (3.1-0-g72492bb), MuTect2 (4.1.8.1), pyClone (0.13.1), Ensembl (release 101, http://ensembl.org/), GraphPad Prism (9.4.1).

For manuscripts utilizing custom algorithms or software that are central to the research but not yet described in published literature, software must be made available to editors and reviewers. We strongly encourage code deposition in a community repository (e.g. GitHub). See the Nature Portfolio guidelines for submitting code & software for further information.

Data

Policy information about availability of data

All manuscripts must include a data availability statement. This statement should provide the following information, where applicable:

- Accession codes, unique identifiers, or web links for publicly available datasets
- A description of any restrictions on data availability
- For clinical datasets or third party data, please ensure that the statement adheres to our policy

The following publicly available data sets were utilised: ExAc (3.1, http://exac.broadinstitute.org), dbSNP (v146, ftp://ftp.broadinstitute.org/bundle), GATK Resource Bundle (hg19/Grch37, ftp://ftp.broadinstitute.org/bundle), Human Proteome (Homo_sapiens.GRCh37.75.pep.all.fa, http://ensembl.org/), IMGT (TCR/HLA, 3.1.17, http://www.imgt.org/), RefSeq (1052019, ftp://hgdownload.cse.ucsc.edu/goldenPath), TCGA (Version 1.0, https://portal.gdc.cancer.gov/), Broad Institute (hg19, ftp://ftp.broadinstitute.org/bundle). The TCR sequences from the present study are available in the article supplemental files, and the genomics data is available on reasonable request from the European Genome-Phenome Archive (EGA) repository (Accession number: XXX)

Human research participants

Policy information about studies involving human research participants and Sex and Gender in Research.

Reporting on sex and gender	Patients were screened and enrolled on this study irrespective of their sex/gender. Any data regarding a patient's sex and gender was collected and provided to the sponsor by the treating physician and PI for the study at each site. No sex- or gender-based analysis has been conducted in this small dataset.
Population characteristics	Provided in extended data table 3.
Recruitment	Patients were recruited across 9 clinical investigational sites. Given the phase 1 nature and complexity of the study, the sites were limited to the United States of America. There were no biases introduced and patients were screened on a first-come first-serve basis based on meeting the protocol inclusion-exclusion criteria. No protocol waivers were allowed on this study.
Ethics oversight	The trial was conducted in accordance with the principles of the Declaration of Helsinki. The trial protocol and statistical analysis plan were designed in a collaboration between the sponsor (PACT Pharma Inc.) and the authors. The protocol was approved by the institutional review board from each clinical site enrolling patients: City of Hope, Duarte California; University of California Los Angeles, Los Angeles California; University of California, Irvine Medical Center, Orange, California; University of California, Davis, Sacramento California; University of California, San Francisco, San Francisco California; Northwestern University Medical Center, Chicago Illinois; Memorial Sloan Kettering Cancer Center, New York, New York; Tennessee Oncology, Nashville, Tennessee; and Fred Hutchinson Cancer Research Center, Seattle, Washington.

Note that full information on the approval of the study protocol must also be provided in the manuscript.

Field-specific reporting

Please select the one below that is the best fit for your research. If you are not sure, read the appropriate sections before making your selection.

☒ Life sciences ☐ Behavioural & social sciences ☐ Ecological, evolutionary & environmental sciences

For a reference copy of the document with all sections, see nature.com/documents/nr-reporting-summary-flat.pdf

Life sciences study design

All studies must disclose on these points even when the disclosure is negative.

Sample size	Up to approximately 76 evaluable participants will be enrolled into the Initial Phase. The planned enrollment for the Expansion Phase study is potentially up to 112 participants, depending on the number and size of the cohorts. The total anticipated enrollment in this study is approximately 9–188 participants. Three to 12 participants will be enrolled into each dose level cohort in the Phase 1a portion of the study. If the study proceeds to the dose-expansion basket cohorts in the Phase 1a, up to 40 additional participants may be enrolled (up to 20 each in the TCR alone and TCR + IL-2 baskets). The dose-escalation stage sample size was based on the probability of not observing any DLTs in 3 participants, and the probability of observing fewer than 2 DLTs in 6 participants for underlying DLT rates during the dose-escalation stage.
Data exclusions	Patients went through a screening process for TCR selection and cell therapy manufacture. Patients were excluded from dosing if they failed eligibility criteria or if a product could not be manufactured. Only products manufactured using version 2.0 or 2.1 were included in the analysis. No primary or secondary endpoint data were excluded from the analysis. All available manufactured products and PBMCs were analysed. Two post-infusion biopsies were excluded from analysis due to insufficient tumour content.
Replication	The NeoTCR-P1 is an autologous TCR therapy manufactured with the patients' own PBMCs and their own unique TCRs. The cell therapies

Replication	were manufactured with up to three independent lots consisting of three unique TCRs or, in some cases, a single TCR, giving technical replicates of the manufacturing for an individual patient. The study included treatment of human participants with a personalized NeoTCR-P1 cell therapy product. Due to the disease characteristics and personalized nature of the cell therapy product, replication of the findings may vary depending on the disease state and the neoTCR selected for infusion. Flow cytometry experiments to analyse the final cell product or post-infusion PBMC samples were performed in duplicate, if there were enough cells available, and all attempts at replication were successful.
Randomization	This was a Phase 1a, open label, 3+3 dose escalation trial design trial design to evaluate NeoTCR-P1 infused as a single agent without or with IL-2, or in combination with nivolumab. Patients were not randomized and were enrolled at the maximum open dose level during the trial, if enough cells were manufactured to meet a given dose level. Once a dose level was cleared, patients and their treating physician had the option to administer the NeoTCR-P1 cell therapy in combination with IL-2. No patients were treated in combination with nivolumab.
Blinding	This was a single arm, open label trial design, thus blinding is not relevant to the study.

Reporting for specific materials, systems and methods

We require information from authors about some types of materials, experimental systems and methods used in many studies. Here, indicate whether each material, system or method listed is relevant to your study. If you are not sure if a list item applies to your research, read the appropriate section before selecting a response.

Materials & experimental systems

n/a	Involved in the study
☐	☒ Antibodies
☐	☒ Eukaryotic cell lines
☒	☐ Palaeontology and archaeology
☒	☐ Animals and other organisms
☐	☒ Clinical data
☒	☐ Dual use research of concern

Methods

n/a	Involved in the study
☒	☐ ChIP-seq
☐	☒ Flow cytometry
☒	☐ MRI-based neuroimaging

Antibodies

Antibodies used	The antibodies used for flow cytometry are detailed in Supplementary Information Table 4. Tumour tissue sections were stained with anti-CD3 (clone EP4426, Abcam; anti-rabbit AF647, ThermoFisher), Vector2A RNAScope Probe to identify neoTCR edited cells (Advanced Cell Diagnostics; Opal 570, Akoya Biosciences, Marlborough, MA), and DAPI (ACD).
Validation	Antibodies used for flow cytometry were validated using human PBMCs, isolated T cells, or activated T cells (activated with TransACT for 48-72 h). Antibodies were titrated and fluorescence minus one (FMO) controls were created to set gates for positive events. For tumour tissue staining, anti-CD3 was protein A purified and validated for IHC on Jurkat (Human T cell leukemia T lymphocytes) cells by the manufacturer (Abcam). The Vector2A RNAScope Probe was validated on FFPE neoTCR edited cell pellets, with un-edited cells used as a negative control.

Eukaryotic cell lines

Policy information about cell lines and Sex and Gender in Research

Cell line source(s)	The SW620 colorectal cancer cell line was purchased from ATCC, and a master cell bank was generated. Cells were transduced to express nucLight red, and further edited to insert an R20Q point mutation in COX6C. Cells were again expanded to generate additional working cell banks.
Authentication	Genotyping confirmed editing but cell lines were not further authenticated.
Mycoplasma contamination	All cell banks tested negative for mycoplasma.
Commonly misidentified lines (See ICLAC register)	*Name any commonly misidentified cell lines used in the study and provide a rationale for their use.*

Clinical data

Policy information about clinical studies

All manuscripts should comply with the ICMJE guidelines for publication of clinical research and a completed CONSORT checklist must be included with all submissions.

Clinical trial registration	NCT03970382
Study protocol	The study protocol, "A Phase 1a/1b, Open-label First-in-human Study of the Safety, Tolerability and Feasibility of Gene-edited Autologous NeoTCR-T Cells (NeoTCR-P1) Administered as a Single Agent or in Combination With Anti-PD-1 to Patients With Locally Advanced or Metastatic Solid Tumors" is provided in the Supplemental Information Files.
Data collection	From December 2019 to February 2022, the study was active at 9 investigational sites: City of Hope, Duarte California; University of

Data collection	California Los Angeles, Los Angeles California; University of California, Irvine Medical Center, Orange, California; University of California, Davis, Sacramento California; University of California, San Francisco, San Francisco California; Northwestern University Medical Center, Chicago Illinois; Memorial Sloan Kettering Cancer Center, New York, New York; Tennessee Oncology, Nashville, Tennessee; and Fred Hutchinson Cancer Research Center, Seattle, Washington. All samples were collected at the patients' investigational site. Data was analysed at PACT Pharma.
Outcomes	Primary Outcomes: 1. Incidence of adverse events as defined as Dose limiting toxicity (DLT): DLT was defined as protocol-defined adverse events that occur within 28 days following infusion of Neo-TCR-P1 administered as a single agent or in combination with nivolumab. 2. Number of participants with adverse events as a measure of safety and tolerability of NeoTCR-P1 or NeoTCR-P1 in combination with nivolumab: Toxicity was classified and graded according to the National Cancer Institute's Common Terminology Criteria for Adverse Events (CTCAE, version 5.0). Cytokine release syndrome (CRS) and neurotoxicity associated with NeoTCR-P1 will be graded according to ASBMT consensus grading. 3. Maximum Tolerated Dose (MTD) of NeoTCR-P1: The MTD was defined as the highest dose with an observed incidence of DLT in no more than one out of six patients treated at a particular dose level. 4. Feasibility of manufacturing NeoTCR-P1: Percent of screened patients that enrolled on study and receive NeoTCR-P1 Secondary Outcomes: 1. Maximum concentration of NeoTCR-P1 (Cmax) in the peripheral blood 2. Area-under-the-concentration-vs-time-curve (AUC) in the peripheral blood 3. Persistence of NeoTCR-P1 in samples of peripheral blood 4. Objective Response Rate (ORR) in participants with solid tumors following infusion of NeoTCR-P1 as a single agent or in combination with nivolumab: ORR was defined as Complete Response (CR) or Partial Response (PR) per RECIST v1.1, as determined by the investigator 5. Duration of Response mediated by NeoTCR-P1 administered as a single agent or in combination with nivolumab to participants with solid tumors: Duration of response, defined as time from the first occurrence of a documented objective response to the time of relapse or death from any cause 6. Progression free survival (PFS) in participants with solid tumors following infusion of NeoTCR-P1 as a single agent or in combination with nivolumab: PFS will be defined from date of administration of NeoTCR-P1 cell infusion to the date of disease progression per the RECIST v1.1 or death as a result of any cause. Subjects who do not meet criteria for progression by the analysis data cut-off date will be censored at their last evaluable disease assessment date 7. Overall survival (OS) in participants with solid tumors following infusion of NeoTCR-P1 as a single agent or in combination with nivolumab: OS will be measured from the date of administration of NeoTCR-P1 to the date of death. Subjects who have not died by the analysis data cut-off date will be censored at their last date of contact.

Flow Cytometry

Plots

Confirm that:

☒ The axis labels state the marker and fluorochrome used (e.g. CD4-FITC).

☒ The axis scales are clearly visible. Include numbers along axes only for bottom left plot of group (a 'group' is an analysis of identical markers).

☒ All plots are contour plots with outliers or pseudocolor plots.

☒ A numerical value for number of cells or percentage (with statistics) is provided.

Methodology

Sample preparation	Peripheral Blood Mononuclear Cells (PBMCs) were collected in ACD or CPT tubes and shipped to Precision for Medicine for PBMC isolation and cryopreservation prior to analysis. Apheresis products were obtained from the patient at the study site and shipped overnight to the study sponsor. After cell manufacture, aliquots of T cells were cryopreserved prior to analysis.
Instrument	Flow cytometry data was collected on an Attune NxT, or cell sorted using a FACS Aria III.
Software	Flow cytometry data was collected using BD FACSDiva (V8.0.8) and analysed with FlowJo (V10.7.1 or V10.8.1), or FCS Express (V6.6.21.0).
Cell population abundance	NeoTCR T cells were single-cell sorted from patient PBMCs using two color staining for neoantigen-HLA multimer CD8+ cells, and were detected at a frequency of >1 in 300,000 CD8 T cells. In the incoming cell product, enriched T cells were greater than 90% pure (determined by CD4 and CD8 staining). NeoTCR+ T cell abundance varied with the starting sample but ranged from 1.9-46.8% of live cells in the final cell product and 0.04-37.3% of live cells in post-infusion PBMCs.
Gating strategy	Gating strategies are shown in Supplementary Information Section. Fluorescence minus one (FMO) controls were created to set gates for positive events.

☒ Tick this box to confirm that a figure exemplifying the gating strategy is provided in the Supplementary Information.